Molecular Level Speciation of Phosphorus in Suspended and Streambed Fluvial Sediments

A Thesis Submitted to the

College of Graduate and Postdoctoral Studies

In Partial Fulfillment of the Requirements

For the Degree of Master of Science

In the Department of Chemical and Biological Engineering

University of Saskatchewan

Saskatoon

By

Mackenzie Wieler

Permission to Use

In presenting this thesis/dissertation in partial fulfillment of the requirements for a postgraduate degree from the University of Saskatchewan, I agree that the libraries of this University may make it freely available for inspection. I further agree that permission for copying of this thesis in any manner, in whole or in part, for scholarly purposes may be granted by the professor or professors who supervised my thesis work or, in their absence, by the Head of the Department or the Dean of the College in which my thesis work was done. It is understood that any copying or publication or use of this thesis/dissertation or parts thereof for financial gain shall not be allowed without my written permission. It is also understood that due recognition shall be given to me and to the University of Saskatchewan in any scholarly use which may be made of any material in my thesis. Requests for permission to copy or to make other uses of materials in this thesis/dissertation in whole or part should be addressed to:

Head of the Department of Chemical & Biological Engineering

University of Saskatchewan

57 Campus Drive

Saskatoon, SK S7N 5A9, Canada

OR

Dean

College of Graduate and Postdoctoral Studies

University of Saskatchewan

116 Thorvaldson Building, 110 Science Place

Saskatoon, SK S7N 5C9, Canada

Abstract

The impact of eutrophication, along with its associated consequences, is an environmental problem around the world. There have been numerous relevant studies and papers that have shown the significance of the correlation between the presence of phosphorus (P) in aquatic environments and the rate and intensity of eutrophication. Although the presence of P has largely been discussed in terms of its effects on the environment and water quality, most of the previous studies have not conducted a thorough molecular characterization of P species found in the suspended sediment contained in fluvial water systems. In this thesis, the importance of P speciation and a more thorough understanding of molecular analysis were discussed and reviewed. Moreover, the characterization methods of X-ray fluorescence (XRF), X-ray adsorption near edge structure (XANES) spectroscopy, and nuclear magnetic resonance ^{31}P-NMR spectroscopy (P-NMR) were used to obtain comprehensive understanding of fluvial sediment samples in terms of their elemental, inorganic P, and organic P distributions, respectively. A significant seasonal influence on P speciation was observed, with an observed increase in the concentration of both organic P compounds and that of iron-associated P during the summer months. Moreover, the concentrations of both orthophosphate monoesters and diesters, including that of phytate and DNA, were also shown to increase consistently during the summer sampling periods compared to spring. Spatial differences were also observed, both in terms of site-to-site comparison as well as catchment inflow versus outflow, although the trends in data were relatively inconsistent when comparing the seasonal differences. The results from this research can be used for a variety of practical applications, such as improving the efficiency of eutrophication control, potential source tracing, and the further development of accurate modelling.

Acknowledgements

I would like to extend my sincerest gratitude towards my supervisors, Dr. Yongfeng Hu and Dr. Hui Wang, for all of their help with both the project and my thesis up to this point. I also need to extend my genuine thanks to Dr. Cade-Menun, who was very accommodating and helpful regarding the work done revolving around NMR analysis, as well as the thesis in general. I would also like to thank the committee members, Drs. Wenhui Xiong and Amira Abdelrasoul, as well as former member Dr. Jian Peng, for their advice and guidance surrounding my research.

I would also like to thank my fellow graduate student, Qingxin Zhang, who provided me with great support and assistance in various aspects of the research and wider scope of the project.

Finally, I also need to thank the project members of the Irish team, Dr. Laurence Gill, Dr. David O'Connell, and Diogo Ferreira, for all their kind support during my time spent working on the project in Dublin, Ireland, as well as their continued support when back at home.

Table of Contents

List of Tables

List of Figures

Nomenclature

Al	Aluminum
BA	Ballynamona
BE	Bunoke
C	Carbon
Ca	Calcium
CLS	Canadian Light Source
CSE	Chemical Sequestration Extraction
DCDA	Dual Culture Diffusion Analysis
DP	Dissolved Phosphorus BA
Fe	Iron
HCl	Hydrochloric Acid
ICP	Inductively Coupled Plasma
IHP	Inositol Hexakisphosphate
LCF	Linear Combination Fit
N	Nitrogen
NMR	Nuclear Magnetic Resonance Spectroscopy
P	Phosphorus
P_i	Inorganic Phosphorus
P_o	Organic Phosphorus
PP	Particulate Phosphorus
Si	Silicon
SSSC	Saskatchewan Structural Sciences Centre

SXRMB	Soft X-Ray Microcharacterization Beamline
TTA	Tintern Abbey
XANES	X-Ray Adsorption Near-Edge Structure Spectroscopy
XRF	X-Ray Fluorescence
XAS	X-Ray Adsorption Spectroscopy
μ-XANES	Micro X-Ray Adsorption Near-Edge Structure Spectroscopy

1 Introduction

1.1 Eutrophication and the Sources of P

When discussing the environmental impact of phosphorus (P), it is important to understand the basics of eutrophication. This phenomenon is caused by an oversaturation of bioavailable nutrients in receiving waters, leading to a higher productivity of autotrophs and an increase in bacterial populations. This then leads to an overall depletion of oxygen and a loss of animal life in the affected environment (Schindler, 1974). This is particularly relevant to this research because the leading cause of eutrophication in non-marine aquatic environments, particularly in lakes, streams, reservoirs, and other freshwater environments, is elevated concentrations of, alongside nitrogen (N), bioavailable P (Ngatia & Taylor, 2018). Phosphorus is especially of concern in freshwater systems because of its role as the major limiting nutrient for algae (Jennings, et al., 2003).

There are other consequences as well, such as loss of water transparency, reduction in fish species diversity, reduction in harvestable fish biomass, and various other concerns related to water treatment (Ansari et al., 2011). Moreover, these phenomena can also have implications on human health, given that people can be affected via digestive, cutaneous, and respiratory means. If someone ingests biotoxins (present in aquatic plants or animals), for example, then they are subject to biointoxication, a disorder identified through pathological conditions. There are also negative economic impacts, as affected areas often see a decrease in tourism revenue, a decline in the fishing industry, as well as suffering the cost of cleaning up the surrounding waters and future mitigation strategies.

However, the main concern about eutrophication is in regard to its environmental and ecological impacts, and there is a growing demand for an increase in the amount of P uptake, or crop uptake, whilst critically minimizing the eutrophication of the affected catchments. The sources of P can, broadly speaking, be divided into point sources and nonpoint sources. Point sources, as the name suggests, describe P contributions from a single place. These may include runoff from various human activities, such as animal feedlots or waste disposal sites, and are often continuous processes that vary little over time. Point sources are also unique in that they can often be accurately traced. Moreover, in some cases, the eutrophication induced from P from point sources can be contained, controlled, and even reversed (Søndergaard et al., 2007).

In contrast, nonpoint sources are much more difficult to identify and trace, as they describe P contributions from various places simultaneously. Examples of nonpoint sources include agricultural runoff pasture or croplands, grazing, and wastewater pollution. Nonpoint sources, particularly that of agricultural impact, contribute significantly more to P loading on a larger scale, and are often seasonally dependent, meaning that they are more dynamic, and difficult, to regulate (US EPA, 2010).

It has long since been known that excessive nutrient loading, particularly from agricultural fertilization, is a major contributor of eutrophication (EPA, 1979). However, this problem still persists today. There was a study that found agricultural nutrient loading leads to excessive concentrations of N and P in the affected aquifers and streams that exceeded standards for water and human health protection (Debruvsky et al., 2010). It has been shown that, in developed countries, the agricultural industry has contributed significantly to the total P discharged into inland waters (FAO, 2011; Jennings, et al., 2003). While there are of course other sources, this is largely due to P being necessary as a component supplied in substantial amounts to agricultural

soils, in order to fulfill its role as an essential nutrient for plant growth and reproduction (Ortiz-Reyes, 2017).

1.2 Phosphorus in Fluvial Systems

Part of what makes this research unique is that it looks at P within the environment of a specific system, namely, suspended sediments within the fluvial catchments that are common in any country with significant agricultural industries. Studying fluvial systems presents unique challenges in the research, such as affecting the sampling processes, the theoretical influences on the speciation, particularly in terms of seasonality, and on the cycling mechanisms, which by extension affect the implications of the results. One of the knowledge gaps, mentioned later in the report, regards the lack of studies conducted within these dynamic systems, relative to more static environments such as lakes and rivers, and makes the study of cycling mechanisms especially difficult to model. The forms and concentrations of exported P can be affected by factors such as stream channel hydraulics and fluvial sediments well before it reaches the site in question. It has been shown that P concentrations, as well as other factors that can have a notable influence on the P uptake, are significantly affected by, among other parameters, the flow regime of the particular catchment (McDowell et al., 2003). Although the modelling of P in static, landscape processes is notoriously difficult as well, it is increasingly more complex when factoring in the dynamic interactions of hydrologic, physical, chemical, and biological processes commonly associated with fluvial environments. The stream flow will change with the seasonal precipitation influences, which will in turn alter the cross sectional area of the channel, the erosion of the banks and rivers will affect the geology of the surrounding water and subsoil

material, and the often biologically dominated P uptake release can be shown to vary greatly in low flow, high temperature systems. All of these concepts must be considered when studying fluvial agricultural catchments and can serve to greatly complicate the already complex task of modelling the P transport. Moreover, there are several factors involved with P in agricultural catchments unique to that of Ireland, to be discussed later in the literature review.

1.3 Eutro-SED Project Outline

It is important to mention that the work done within the scope of this thesis is actually a smaller part of a larger project, known as Eutro-SED. The objective of this project is to examine eutrophication hotspots resulting from biogeochemical transformations and bioavailability of phosphorus in the fluvial suspended sediment of geologically contrasting agricultural catchments. Put more simply, to study the relative importance of suspended and streambed sediment bound P.

This venture is something that can only be accomplished through a multiple team effort, in this case teams in Canada, Ireland, and Sweden, all of whom have varying and overlapping responsibilities involving sampling, analysis, and modelling. The role of the Canadian team, and by extension the work done in this research has been focused on the advanced spectroscopic analysis of the soil samples, detailed later. This is conducted after sampling and initial analysis has been performed, and after completion, the samples and data are given to the Swedish team, which will focus on the development of modelling and mechanisms. Both Trinity College Dublin and the Swedish University of Agricultural Sciences served to develop, design, and run fluvial suspended sediment sampling campaigns under fluctuating flow and redox conditions, and to

produce comprehensive reaction networks that define the behaviour of P in redox-dynamic fluvial sediments. Also worth mentioning is that this research specifically concerns sediments extracted from fluvial environments, unique to other studies which have primarily focused on more static aquatic environments, such as lakes and reservoirs, as well as, or in addition to, agricultural soils.

1.4 Research Objectives

The extensive research carried out by Jennings et al. (2003) identified several knowledge gaps that need to be addressed in research industry. Relatively little research has been done to ascertain the temporal and spatial influences of particulates and sediments on bioavailable P in fluvial systems affected by agricultural run-off. Less emphasis has been placed on the development of accurate models especially concerned with P relative to other nutrients or pollutants, such as N and pesticides. These knowledge gaps have led to the research objectives, which have remained relatively unchanged throughout the project, outlined below:

- To examine and understand the molecular characterization of P found in fluvial environments within agricultural catchments
- To study the seasonal and spatial impact on sediment P speciation in fluvial systems within agricultural catchments
- To contribute to the further understanding of fluvial sediment-associated P speciation dynamics for the eventual development of accurate models

- To demonstrate the advantageous complimentary nature of combining advanced spectroscopic techniques, including ^{31}P-NMR and XANES to gain more comprehensive knowledge on organic and inorganic P speciation and dynamics

Part of this project, and by extension the research conducted within the scope of this thesis, seeks to address these issues specifically. This is accomplished through advanced spectroscopy analyses, including X-Ray Adsorption Near-Edge Spectroscopy (XANES) and ^{31}P nuclear magnetic resonance (^{31}P-NMR) spectroscopy, were performed in Canada, at the Canadian Light Source (CLS) and Saskatchewan Structural Sciences Centre (SSSC), respectively. The reason why these more advanced materials analysis techniques are necessary is because the simpler, more widely-used techniques, like chemical sequential extraction (CSE), yield less precise results. By using more specialized, focused spectroscopic methods, we are able to produce much more precise and significant results. This is especially true for the molecular speciation of P, wherein these advanced techniques are particularly useful.

All of these techniques, detailed later, have been utilized in similar past projects (Glæsner et al., 2019; Wei et al., 2019; Liu et al., 2017), but have only recently been regularly used together, and not in this context, which provides meaningful conclusions. Though it is also important to note that more studies are needed before the speciation and characterization of P on a molecular level can be fully understood. This enhanced knowledge will assist catchment scientists in the adoption and development of better land management policies, which will serve to reduce nutrient inputs and, in turn, reduce the impact of eutrophication on freshwater ecosystems, including agricultural streams and rivers.

1.5 Thesis Outline

The content of this thesis details a comprehensive review of the analytical techniques of XRF spectroscopy, P K-edge XANES spectroscopy, and ^{31}P NMR spectroscopy, in order to thoroughly understand the molecular speciation of fluvial sediment samples. The motivations behind this research, and broader associated problems in general, are introduced and discussed in terms of the work conducted. The first chapter describes the project and research in general terms and serves to outline the thesis, the second chapter provides a literature review of the background knowledge needed to understand the concepts of the research, describing the relevant concepts, advantages, and issues associated with each method of analysis. The third chapter details the methods of experimentation used in this study, while the fourth chapter presents, and thoroughly discusses, the research results. Finally, in the fifth chapter, the conclusions of the data are reviewed and recommendations for future work are made before the thesis is summarized.

2 Literature Review

2.1 Relevant Forms of Phosphorus

There has already been extensive work conducted surrounding the understanding of different P forms, which has helped to outline the ways in which P can be classified. Phosphorus is often delivered to agricultural catchment systems as a mixture of dissolved and particulate inputs, each of which is a complex mixture of different molecular forms of P (Jennings, et al., 2003). Most commonly, P can be categorized both physically and chemically. Physically, P is often operationally defined in four different forms: particulate phosphorus (PP), dissolved phosphorus (DP), colloidal P, and truly dissolved P. Though the latter two of which are significantly less frequently identified in agricultural runoff than that of PP and DP. These forms, as suggested to avoid subjective terminology are defined based on the filter sizes used to measure them, with PP retained on a 0.45 mm filter, dissolved P on a <0.45 mm filter, colloidal P on a 0.2-mm filter, and truly dissolved P on a <0.2 mm filter. Relatively little is known about the chemical forms, which can be broadly classified as either organic phosphorus (P_o) or inorganic phosphorus (P_i), both of which are found in both PP and DP.

Organic P forms are often classified into the following pools: orthophosphate esters, phosphonates, and anhydrides. Orthophosphate esters are categorized based on the number of ester groups linked to each orthophosphate. This is typically seen as either mono- or di-, but tri- exists synthetically as well. These are also normally stable in the pH range of most soils. However, they may also hydrolyze readily in extreme pH or from phosphatase enzymes (Corbridge, 2000). Orthophosphate monoesters are the most dominant form of P_o in most soils, and are mostly made up of inositol phosphates in a variety of stoichiometric forms.

Orthophosphate diesters include nucleic acids, phospholipids, and teichoic acid. Phospholipids, typically major components of cell membranes, include, among many others, phosphatidyl choline and ethanolamine. Nucleic acids, either DNA and RNA, consist of sugar molecules connected to orthophosphate. In soil, DNA exists as chromosomal DNA in linear form and supercoiled plasmids (Poly et al., 2000; Corbridge, 2000).

Phosphonates, unlike other P_o forms, contain the C-P bond. Phosphonates also only tend to accumulate in soils with few organisms containing phosphonates enzymes. These conditions are typically wet, cold, or acidic (Hawkes et al., 1984).

Inorganic P forms may be present as minerals, sometimes classified as primary and secondary minerals, or absorbed onto surfaces. Relevant to soil P, apatite is typically the most commonly occurring P mineral found in ordinary sediments, particularly in soils of low acidity. Phosphate may also be present in the form of Fe or Al phosphate oxides, or combined with metals such as Al, Fe, or Ca to form secondary minerals (Blaise, Venugopalan, & Singh, 2018). These forms are often considered to contribute little to the mobilization of DP, with absorbed orthophosphate P thought to be the primary inorganic P contributor. Finally, orthophosphate anhydrides are found, in trace amounts, as polyphosphates found in bacteria fungi, algae, protozoa, insects, actinomycetes (Kulaev, 1979).

2.2 P in Irish Agriculture Catchments

Broadly defined as any area of land surrounding a body of water, such as rivers or lakes, catchments are very common systems when studying the effects of eutrophication. With the essential role P plays in fertilizers as an important stimulant for plant growth, the concept of P in

agricultural catchments continues to be increasingly relevant and important. Continual application of fertilizer has been shown to increase the amount of plant available P (Tunney 2000). Naturally, the type of farming will go on to affect the rates of fertilization, which will in turn affect the P loading contributions. By extension, the type of environment will affect the type of farming performed, with the types of soil, weather, temperature, etc., being particularly important factors.

In the context of this research, the system being studied is that of catchments in Ireland, which possess unique traits that need to be considered. Firstly, being a largely agricultural country, farming accounts for approximately 60% of land use in the Republic of Ireland, the vast majority of which consists of grass agriculture (CSO, 2010). There was a study conducted by Zhang et al. in 2008 that showed through geochemical mapping the importance of soil characteristics influencing labile P in Irish agricultural lands. There have been a lot of studies conducted on Irish agricultural catchments, most aimed at minimizing P loss and improving land management practices. Currently, P fertilization (chemical or manure) in the Republic of Ireland is governed by the Good Agricultural Practice for Protection of Watersheds Regulation (2010), which uses a soil P index based on P concentrations in Morgan's extract (sodium acetate and acetic acid). This value, known as the Morgan's P value, is used to determine the rate of P fertilizer that can be applied to a corresponding soil, adjusted for land use, based on a soil index Morgan's P. If values exceed an upper threshold (8 mg L^{-1} for grasslands; 10 mg L^{-1} for other crops), no additional P fertilizer can be applied. Morgan's P measures labile P in soil. When there is more labile P present in the catchment soil, there a corresponding increase to the reactive P loss in the surface runoff (Tunney et al., 2000; Regan, Fenton, Healy, 2012).

2.3 The Transformation and Transport of P

One of the reasons environmental P can be so difficult to study is because P compounds can undergo what is known as cycling. The concept of environmental P compound cycling describes the intricate process in which the P compounds in a given system will transform from non-labile to labile, becoming available for plant uptake, or the reverse. The dynamics and mechanics involved in P cycling are incredibly complex and will vary greatly depending on the soil characteristics, inorganic and organic forms present in the system, and a variety of other environmental factors. There are a number of individual processes involved in P cycling: dissolution-precipitation, sorption-desorption, mineralization-immobilization, and oxidation-reduction of P, all of which play a vital role in the transformation of soil solution P (Pierzynski, McDowell, & Sims, 2005).

Generally speaking, most of the P in soils originates from the dissolution of common minerals within the soil, primarily apatite, into phosphate within the soil solution. However, as the minerals continue to weather, Al and Fe phosphates may be increasingly prominent as well. Sorption and desorption reactions occur when phosphates attach to the surfaces of the hydrous oxides, clay minerals, and carbonates present in the system, serving to equilibrate with the soil solution. P_i and P_o forms also play a key role in the adsorption to the soil minerals, and the classification of orthophosphate esters can serve to influence the kinetics, with orthophosphate monoester adsorption being slower and more temperature dependent than that of orthophosphate diester adsorption, though little is known regarding the latter (Shang et al., 1990). Precipitation, a process by which the P reacts with another substance, commonly for those containing the aforementioned minerals, to form another solid mineral, particularly when soluble P fertilizers

are introduced. Immobilization describes the biological conversion of P_i into P_o, while mineralization is the process of P_i becoming released into the system from soil P_o.

In regard to the involved kinetics, and by extension the modelling, the interactions of P compounds and the environment are often quite complex, and will vary greatly depending on numerous factors. First, most of the work done so far has been focused on static aquatic environments, such as lakes and reservoirs. Far less research has been conducted on the kinetics involved in fluvial environments, such as streams and rivers, as it can be much more difficult to provide a reliable model for eutrophication or P cycling mechanisms. That being said, even kinetic analysis of static environments proves to be quite challenging, citing variability among temporal, spatial, temperature, light, and nutrient variety/concentration as major concerns for dependable and reliable modeling (FAO and WHO, 1995).

Finally, when speaking to P compounds present in the system and the cycling mechanisms involved, it is also important to consider the difference between high flow and low flow systems. Moreover, this is also a factor from a seasonality standpoint as well, as the summer months will typically see lower flow than that of the spring. Fluvial stream ecology may be impacted by changes in stormflow and baseflow that are associated with varying sampling periods experienced throughout the year, which can greatly affect the concentration of P present in fluvial environments (Shore et al., 2017). To this point, there have been studies that have found that total reactive P concentrations increase during periods of lower flow, such as the summer months (Vero et al., 2019).

Summarily, there are a number of biological, chemical, and physical factors that can affect the transformation of P compounds in the environment, including that of soil and water. These factors include significant environmental conditions, such as temperature or land use. The fact

that the soil P cycling heavily depends on the P forms in the system further highlights the benefit of reliable and accurate speciation techniques.

2.4 Methods of P Analysis

There are, of course, many different analysis techniques currently being utilized to study and measure P in soil, providing useful information about the P concentrations, forms, and other related data about the environmental samples. They tend to vary greatly in terms of accessibility, accuracy, and in the type of data they provide.

2.4.1 Methods for Determining P Bioavailability

Given the importance of agriculture, there have been many soil P tests established and used to determine and estimate the bioavailability of soil P. These tests will be used to guide recommendations given to farmers, in order to regulate the nutrient loading being applied to croplands, and tend to vary based on which country the tested soil is in. Most common among these techniques is the molybdate blue method, which determines P bioavailability through calculating the orthophosphate in the solution (Riley, 1962).

There is also what is known as dual culture diffusion analysis, which is a procedure used to analyse the algal bioavailable P in suspended and particulate P. Broadly speaking, the experimental procedure involves the use of an apparatus of two tanks separated by a membrane (DePinto, 1981). This experiment is used to analyze the bioavailability of phosphorus, as well as the impact of seasonality on P releasing dynamics of the sediments. This technique was critical

to work done within the broader scope of the project (Zhang, 2020), but is not overly relevant to the work conducted within the scope of this thesis, and will not be discussed in further detail.

Currently, there are no direct methods for determining the concentration of total organic soil P, instead estimating the P_o through means of extraction and ignition, both of which possess unique advantages and disadvantages over one another. Both methods can misestimate the actual organic P concentration in the soil samples, and it has been found that orthophosphate calculated in alkaline extracts was consistently lower than that determined by ^{31}P NMR spectroscopy, likely due to orthophosphate becoming complexed with organic matter in the extract solution (Turner et al., 2003). Ignition methods involve the ashing of all organic matter in the sample, either utilizing high or low temperatures, and then calculating the total P_o concentrations based on the difference between the remaining P_i in the ignited sample and the original unignited material (Kuo, 1996). Extraction methods however, determine P_o in the extract, both before and after oxidation, through digestions using acids, bases, or a combination of both. The remaining extracts can then be analyzed through different techniques.

One of the more common methods used in this overall project is chemical sequential extraction (CSE). This is used as a common technique for separating the different P pools based upon solubility in a series of extractants. The first comprehensive sequential extraction method for soil P was established by Chang and Jackson in 1957, which has since been extensively used and heavily modified by others. For example, the research done by Jensen and Thamdrup (1993) has facilitated an established CSE method for P in freshwater environments. For this project, Zhang (2020) used the following series of extraction steps on sediment samples: First, milli-Q water was used to extract the loosely-bound phosphate. Second, bicarbonate dithionite (BD) solution was used to extract reductant-soluble P, which is here assumed to be iron/manganese-bound P.

Third, NaOH solution was used to extract both aluminum oxide-bound P and organic P (some of the extract will be further digested by $K_2S_2O_8$ to calculate the organic phosphorus, P_o). Fourth, HCl solution is used to extract acid-extractable P, here considered to be calcium-bound P. Finally, the residual sediments are digested in concentrated HCl solution to determine residual P. The solutions extracted by the steps listed above are then analyzed using colorimetry in Konelab, an automated, clinical chemical analyzer. This technique is widely used in laboratories partially due to the availability, and while it can provide some useful information regarding P solubility, fractions are operationally-defined and therefore are imprecise, and it does not provide the detailed molecular characterization as will be obtained with more advanced spectroscopic techniques.

2.4.2 Methods for Determining Total P Concentrations

Another method of P analysis is inductively coupled plasma (ICP) atomic emission spectroscopy, which can be used as a method for determining the elemental concentrations within a soil solution extract. This process can be generalized as using a spectrometer to ionize the samples, creating both atomic and small polyatomic ions, which are then detected by the instrument and processed as concentration data. This process is particularly effective in the detection of metals within a specific atomic mass range. After digestion of the solids, this technique can provide information on total atomic concentrations and the detection of trace elements in the soil samples. Unlike more common colorimetric techniques used to analyze soil P extracts, ICP is also able to detect the total P in the solution. However, in the context of this

project, this method is primarily used as a prerequisite for NMR spectroscopy, which is a more accurate form of analysis that will be detailed later.

X-Ray Fluorescence (XRF) analysis is a radiation-based technique that utilizes the excitation of an atom within the sample, in order to measure the fluorescent energy emitted by the electron. This method serves to provide an elemental distribution of materials. However, it is not chemically sensitive and often lacks the accuracy of more advanced techniques. While most XRF experimentation can be preformed in routine laboratories, it may also be conducted with the use of the beamline from advanced facilities, which allow for a tunable energy source unique to most practices of the technique. By measuring this over a range of energy levels, the generated spectrum, represented by the different excitation levels, will correspond to specific elements and thus provide information about the elemental distribution of a sample.

2.4.3 Methods for Determining P Speciation

Of course, all of the methods mentioned previously can only give a limited degree of detail, and are unable to show the molecular level speciation of P compounds present in the soil and other environmental samples. In order to speciate P, more advanced methods must be used. These methods include P K-edge XANES spectroscopy, and ^{31}P NMR spectroscopy, both of which will be discussed in the sections to follow.

These methods are unique to one another in that, while XANES can be used to study organic P compounds in some cases, it is shown to be more sensitive for inorganic P compounds because the P K-edge XANES spectra for most organic P species are fairly similar and featureless. This is where NMR spectroscopic analysis is particularly useful, considering that XANES analysis

can struggle with differentiating between organic P compounds that NMR is reliably accurate with. NMR spectroscopy helps to cover the disadvantages associated with XANES, as it possesses accuracy with the organic P compounds (Mishra, 2017). Complimentarily, ^{31}P-NMR also tends to struggle with differentiating between inorganic P associated compounds, relative to other standards used.

2.4.3.1 X-Ray Adsorption Near Edge Spectroscopy (XANES)

In comparison to simpler chemical extraction methods to characterize general P pools, P K-edge XANES analysis is a more advanced, radiation-based technique for P speciation. This technique is direct, non-destructive, and has a wide variety of applications that goes beyond that of sediment-bound P characterization. The synchrotron operates by accelerating electrons, up to nearly the speed of light, along a path into a storage ring, wherein the electron is bent via a magnetic field. This beam emits radiation tangentially along the beamline, which can then be used in endstations or with separate experimentation techniques over a wide range of photon energies. This process is useful because in addition to measuring the energy in fluorescent light, it also measures the energy of photoelectron and Auger electron. When the photoelectron is excited from the incoming x-ray, it creates an unstable core hole which is filled by a valance electron, which then in turn produces an Auger electron from the excess energy. Because the energy is recorded over a wide range of photon energies, the spectra generated includes pre edge structure, near edges structure, known as X-ray adsorption near edge structure (XANES), and extended adsorption edge structure. The XANES spectra, referred to by the specific electron that is excited and which core orbital loses the electron (for example P 1s electron in P K-edge), is

particularly useful in that it provides information about valence state and bonding (Kelly et al, 2008).

Somewhat similar to the bulk XANES analysis, μ-XANES is another useful tool when determining the full speciation of a sample. Normal bulk XANES analysis, as useful as it is, is only able to provide information on the sample representative of the average concentration over a relatively large area. μ-XANES is able to analyze the sample heterogeneously, probing areas of interest within the sample and showing elemental correlations that would otherwise remain unseen. By focusing the beam in one spot within the sample, the localized chemical composition can be determined from the near-edge spectrum in an area smaller than 0.2 μm by 0.2 μm (Zhang et al., 1994). In the context of this research, μ-XANES analysis can serve to improve the detection and identification of minor P species in the soil samples, and using spectroscopic analysis at different scales, both macro and micro, helps to connect P speciation with mobility of P in soils (Hesterberg et al., 2017). Moreover, the spatial distribution can be seen through image mapping the sample based on absorption maxima of specific chemical bonds, providing a contrasting look into the chemical constituents important to the sample composition. This is particularly useful as this method focused on a subset of various components within the soil which are expected to produce spectra with contributions from fewer species. If there is a relatively large amount of P species in a sample, then more of these species should be identifiable across multiple, more focused scale locations within said sample. XANES is limited in the sense that the theoretical number of P species grows drastically when considering the multitude of factors/variables in the chemical environment. The spectra generated must be representative of the soil matrix present within the sample, and by utilizing different scales

within XAS, this allows for the improvement in the identification of diversity of P species with a relatively high degree of certainty.

Relatively speaking, XANES analysis is very detailed, detecting specific compounds that other processes cannot. That level of detail associated with XANES spectroscopy is relatively very high and can be used to great effect when understanding the complete speciation of a sediment sample. Comparatively, P K-edge XANES analysis is more sensitive to inorganic compounds than similar methods, such as ^{31}P-NMR. This is because the effectiveness of differentiating between chemical species is largely dependent on the uniqueness of the features in the standard spectra analyzed in Linear Combination Fit (LCF) analysis (Kelly et al., 2008).

2.4.3.2 ^{31}P Nuclear Magnetic Resonance (NMR) Spectroscopy

Another more advanced method of molecular analysis is nuclear magnetic resonance spectroscopy (NMR). Unlike P K-edge XANES, which is performed in solid state in this project, ^{31}P NMR can be conducted in either solid state or liquid state (more commonly called solution P-NMR). This is an advanced spectroscopic technique that may be applied to differentiate groups of P based on the response of the sampled nuclei under the influence of electromagnetic radiation and a magnetic field. It is because of this field that the spinning nuclei orient themselves either 'toward' or 'against' the field. The difference in energy levels between these two states can be measured as a net energy adsorption, when the correct electromagnetic radiation frequency is implemented, causing the lower energy level state to flip to that of the higher energy level state. The exact amount of energy required for this 'resonance' will depend on the strength of the field and the nuclei being examined (Pierzynski et al., 2005). This measured response, in the form of

the resonant frequency of the nuclei, is then recorded as a chemical shift in ppm. An example of this generated spectra can be seen displayed in Figure 1 below.

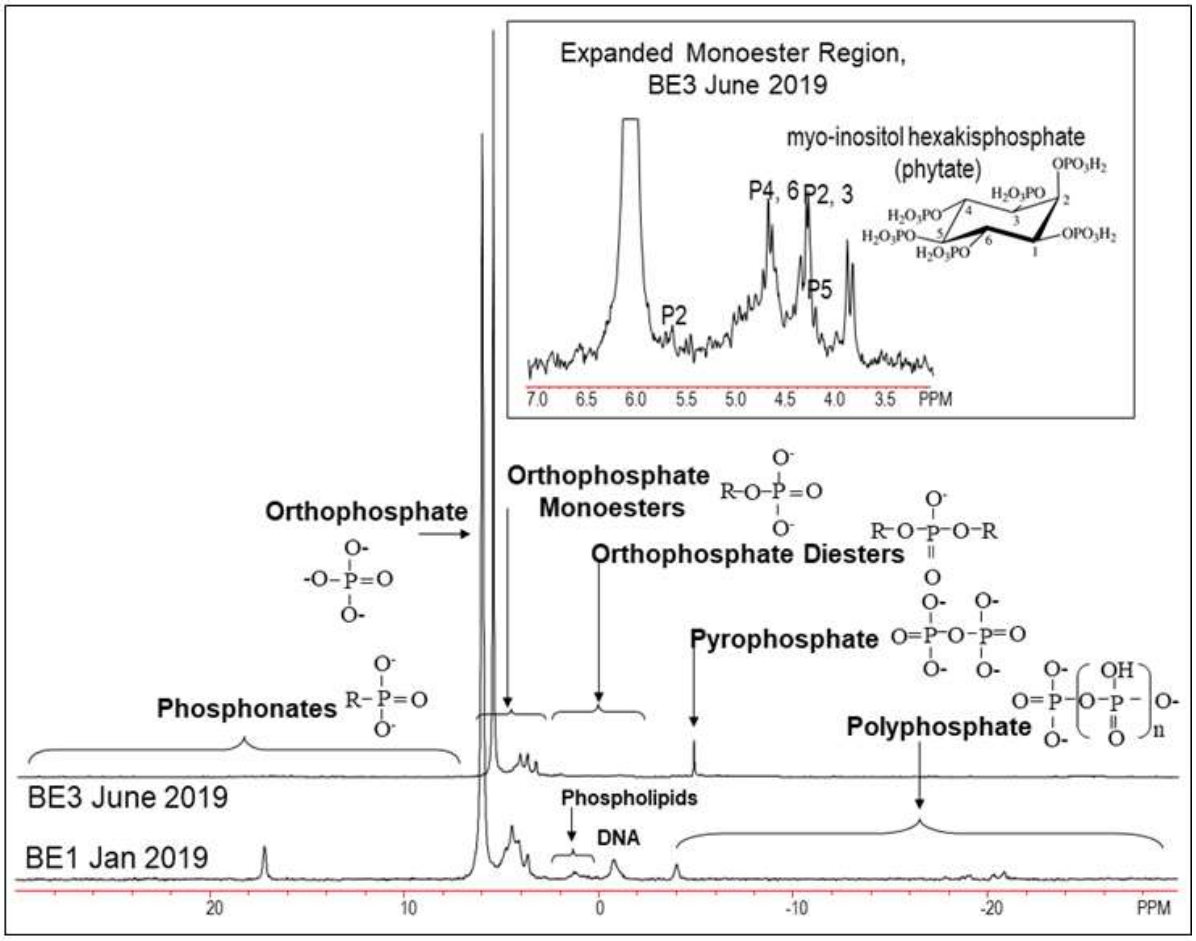

Figure 2.1: ^{31}P-Nuclear Magnetic Resonance (NMR) spectra of stream sediments extracted with NaOH–EDTA for BE3-Jun19 and BE1-Jan19 samples

Unlike most other forms of spectroscopy, NMR requires a magnetic field and concerns the nuclei rather than the electrons (Canet, 1994). This technique is commonly used in diverse fields because of its versatility in studying structure and interactions across a variety of molecular systems, which is often applicable to environmental studies (Simpson, 2018). In the context of this research project, the nuclei in question will be ^{31}P, which possess unique advantages, due to

^{31}P retaining an abundance of 100%, as well as a relatively high gyromagnetic ratio (Mishra, 2017). Samples from this study were also 'spiked', after the initial analysis, with certain compounds such as phytate, to confirm peak identifications, as the chemical shift will vary from one sample to another, and is affected by the sample matrix.

2.5 Section Summary

The literature review in this chapter is intended to serve as a proper introduction to the relevant topics involved in the research, and to provide the appropriate background knowledge necessary to understand the results better.

Eutrophication, caused in large part due to excessive P concentrations, leads to environmental and ecological concerns that need to be addressed through the better understanding of P characterization within the suspended soil on a molecular level. There are common analysis techniques that are able to show limited information of P present in the system, but they are unable to show the molecular level speciation necessary to understanding the complex and difficult nature of the soil. In order to accomplish this, several techniques can be used alongside one another. Namely, P-XANES and solution P-NMR analysis are able to provide a complimentary and detailed view into the speciation of the involved soil samples.

3 Methods of Experiment

In this chapter, various processes and methods will be outlined and detailed to give an appropriate indication as to how the research was conducted and the data was collected. These include selection of the sample sites where the samples were extracted, the sample extraction itself, the relevant initial analysis techniques (in particular CSE), as well as the more advanced spectroscopic techniques of XANES and NMR analysis.

3.1 Sampling and Site Selection

Although the broader project uses a wider range of sampling sites in Ireland, only selected locations were analyzed within the scope of this thesis. Samples were collected from three sites located in different regions in Ireland: Tintern Abbey (TTA), Ballynamona (BA), and Bunoke (BE), as shown in Figures 3.1, 3.2, and 3.3 below. These catchment sites were chosen due to their highly eutrophic water, their varying surface soil composition, as well as being listed by the Irish Environmental Protection Agency (EPA, 2018) as being areas of concern, all of which make them ideal locations to compare and contrast spatial influences on eutrophication, through the use of molecular characterization.

Tintern Abbey is the smallest of the sampling sites, at a watershed area of around 10 km^2. Its parent surface soil material contains river alluvium, fine loamy drift with limestones, and siliceous stones. Its geology largely consists of shales, sandstone and limestone tills. It also shows shallow poorly draining soils. In terms of agriculture, this site's land use consists mainly of pasture-based agriculture with some tilled cropland and woodland. The Ballynamona watershed size is about 20 km^2, with parent soil composition of river alluvium, limestone till, and

karstified limestone bedrock. Finally, Bunoke has a watershed size of around 15 km^2, and its parent surface soil material consists of river alluvium, sandstone till, shales and sandstones till (Namurian), and heavy, carboniferous limestone till. Both Ballynamona and Bunoke have pasture-based agricultural land use.

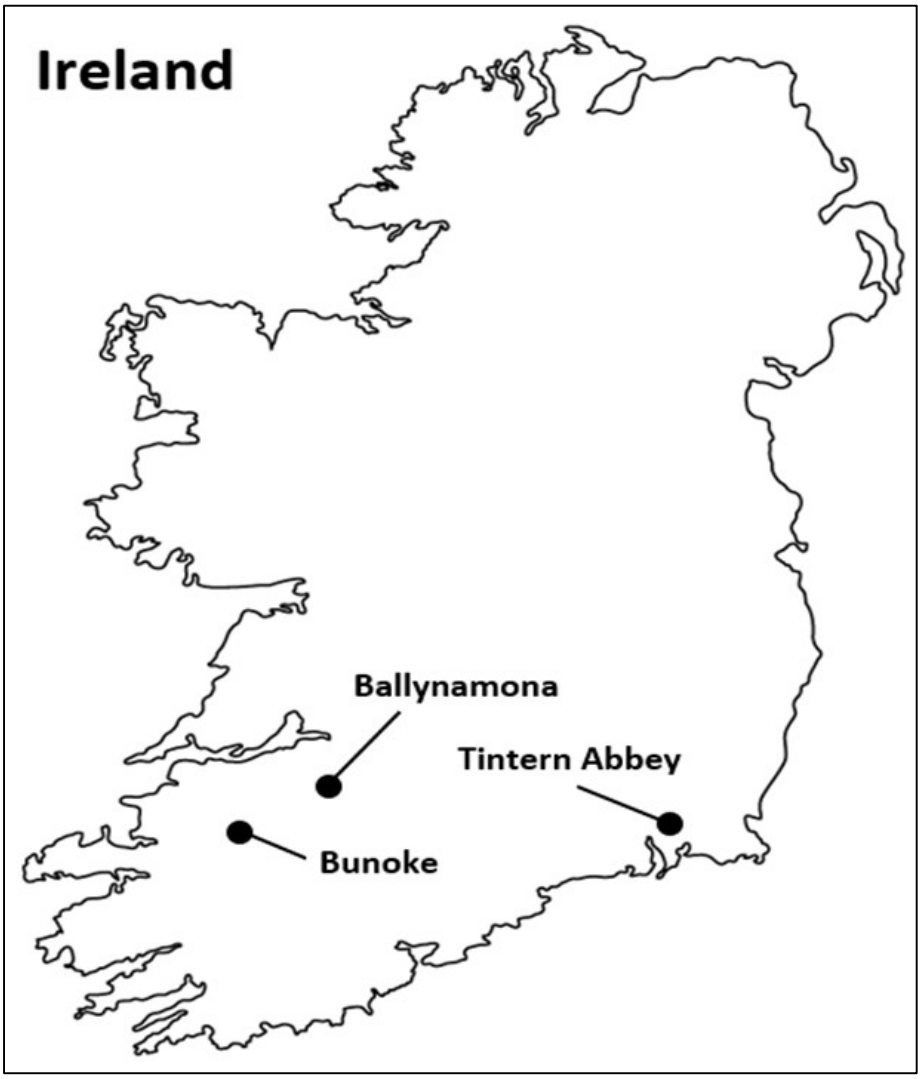

Figure 3.1: Ballynamona, Bunoke, and Tintern Abbey Catchment Field Sites in Ireland

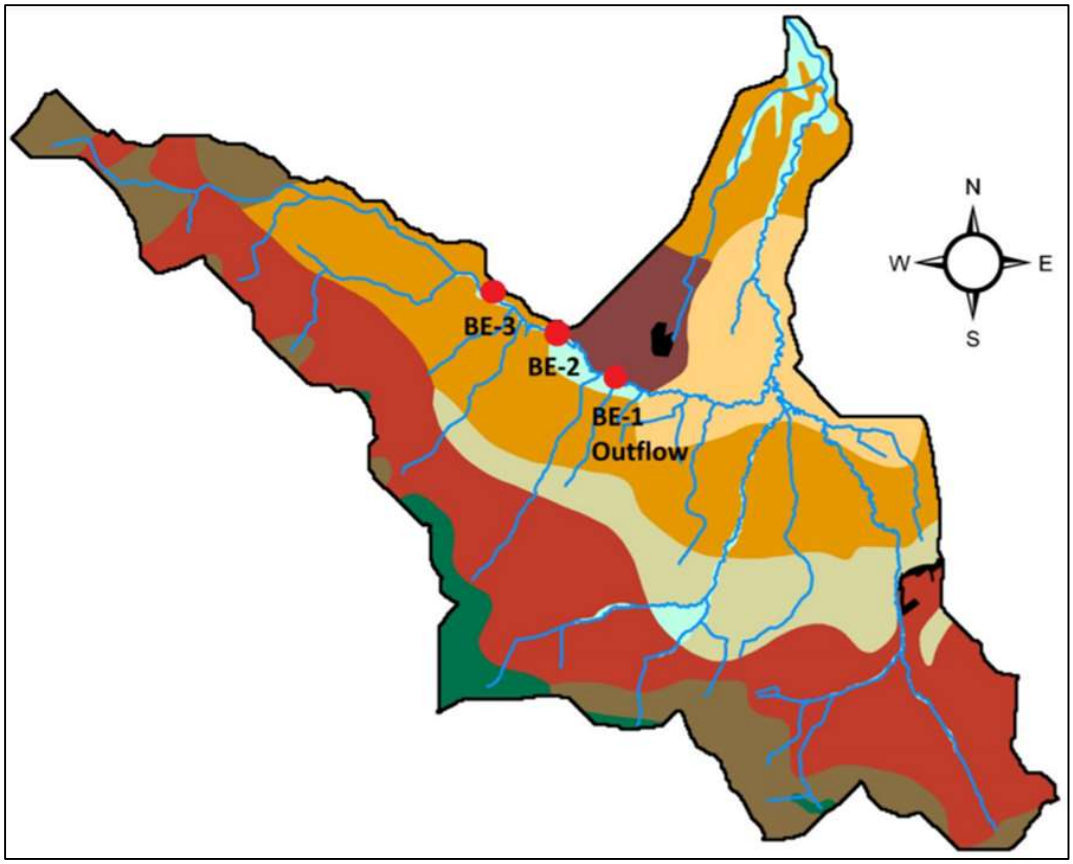

Figure 3.2: Intrasite Catchment Location Map for Bunoke Sample Site (Courtesy of Dr. David O'Connell, Trinity College Dublin)

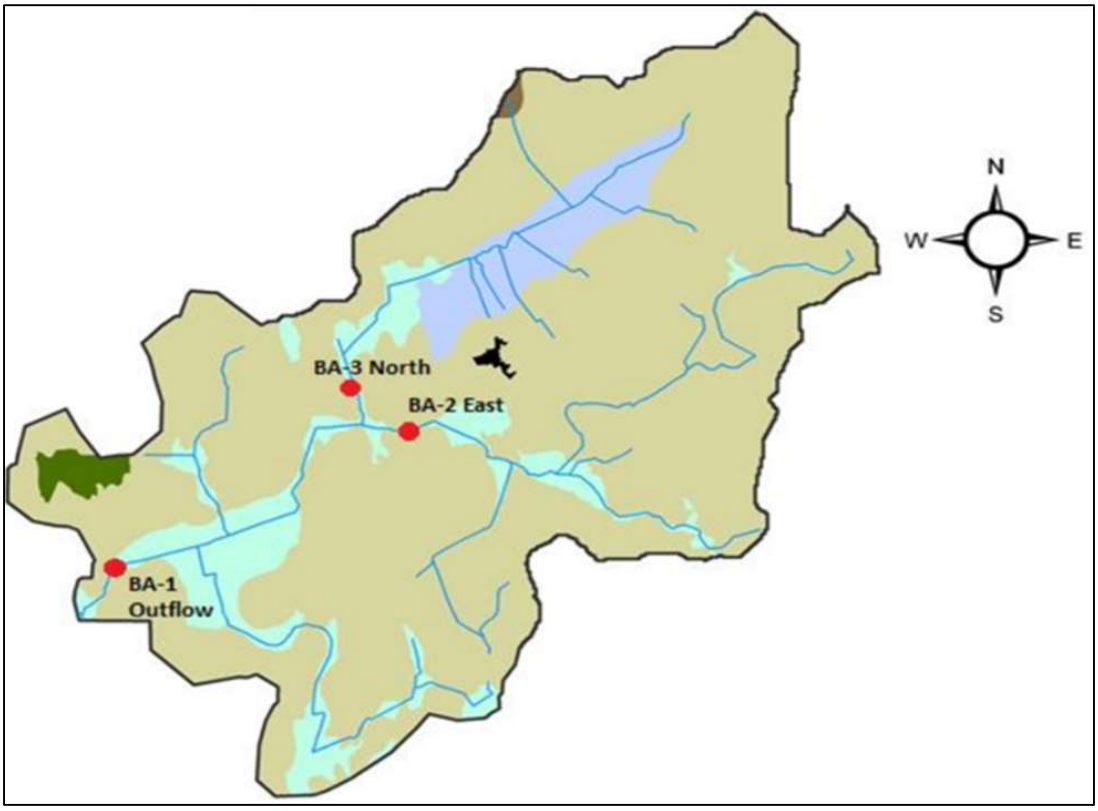

Figure 3.3: Intrasite Catchment Location Map for Ballynamona Sample Site (Courtesy of Dr. David O'Connell, Trinity College Dublin)

The sampling catchments also show significant and relevant differences in the seasonal impact they experience throughout the year. Appropriate weather data, collected from nearby weather stations for the relevant catchment sites over thirty-year periods, has shown a significant difference in the amount of average rainfall that each site experiences. Moreover, these data clearly show the months with increased or decreased precipitation, which is generally consistent from site to site. A table of these data, as well as a comparative graph, can be found summarized in Table 3.1 and Figure 3.4 below.

Table 3.1: Weather Data for BE/BA, and TTA Sampling Sites

	Shannon Airport (1981-2010) (BA and BE Sites)		**Rosslare (1978-2007) (Tintern Abbey Site)**	
	Temp (°C)	**Rainfall (mm)**	**Temp (°C)**	**Rainfall (mm)**
Jan	6	102.3	6.5	88.4
Feb	6.2	76.2	6.3	70.8
Mar	7.8	78.7	7.5	69.1
Apr	9.5	59.2	8.8	59.1
May	12.1	64.8	11.1	55.7
Jun	14.6	69.8	13.6	54.9
Jul	16.4	65.9	15.5	49.9
Aug	16.2	82	15.7	71.6
Sep	14.2	75.6	14.2	75
Oct	11.2	104.9	11.6	109.3
Nov	8.3	94.1	9	100.9
Dec	6.3	104	7.4	100.8
Year	**10.7**	**977.6**	**10.6**	**905.5**

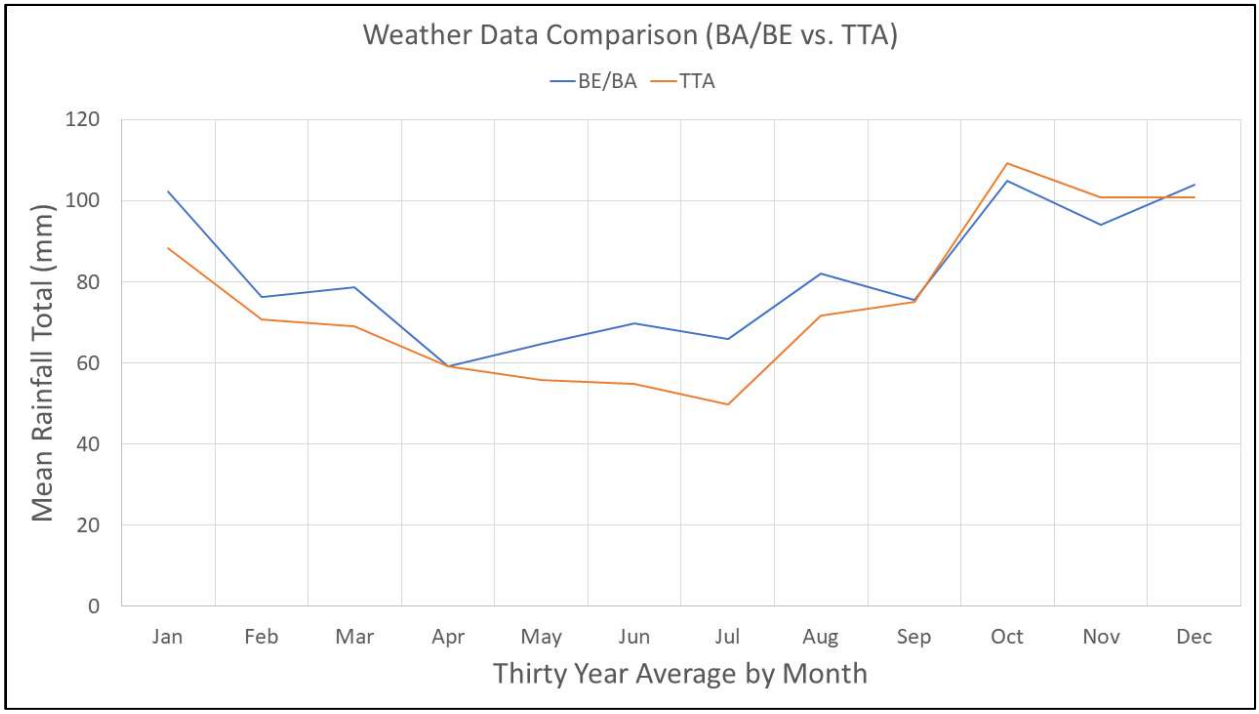

Figure 3.4: Rainfall Comparison for BA/BE and TTA Sampling Sites

Fluvial sediment samples were manually collected with Phillipe sediment traps (Zhang, 2020). These samplers work by dramatically slowing down the water velocity, to promote deposition, before final collection is possible. With these traps, stream suspended solids were gathered periodically over different time periods of both high flow and low flow. The contents of the Phillipe sediment traps were then carefully transferred into 10L containers and transported back to the lab, whilst maintained at around the stream temperature, where they were stored in a refrigerator before initial processing. A more detailed description of the sampling can be found in the Appendix.

In addition to the fluvial sediment samples, surface water samples were also collected using water samplers at the outflow areas in each catchment site. These water samples were collected into plastic bottles, kept cool, and moved to the laboratory where they were vacuum-filtered and stored for other analyses. In addition, there were water-level loggers, as well as weather stations, to assist in quantifying the seasonality of the catchments, such as measuring and analysing the magnitude of the precipitation.

Finally, the collected samples were put through a series of preparation and initial analysis steps, before further analyses. This pre-processing of each fluvial sediment sample included wet sieving, centrifugation, and decantation of the supernatant, followed by freeze-drying of sediment samples. Outside of this research but within the project, some of the samples were also analyzed using CSE analysis, DCDA processing, and ICP analysis.

3.2 Advanced Spectroscopy Methods

As previously mentioned, the advanced spectroscopic analytical techniques are that of XANES and NMR analyses. XANES analysis section includes the XRF analysis, the bulk XANES, and the μ-XANES.

3.2.1 X-Ray Adsorption Near-Edge Structure (XANES)

Both XANES spectroscopy and XRF spectroscopy were conducted at the Canadian Light Source under the supervision of Dr. Hu. The XRF measurement was conducted using the soft X-ray microcharacterization beamline (SXRMB) at a photon-energy of 7200 eV. These signals were then recorded and normalized over a wide energy range before being overlaid for appropriate comparison. Similarly, the XANES measurement was also done using the SXRMB beamline and processed with the Athena software (Ravel & Newville, 2005). The linear combination fit (LCF) analysis of the generated spectra was performed using the reference standards of $FePO_4•2H_2O$ for iron, $Ca_2(PO_4)_3$ for calcium, and *myo*-inositol hexakisphosphate (*myo*-IHP, phytate) bound to various compounds (Si, Ca, ferrihydrite) as a proxy for organic P. The individual spectra for these reference standards can be found in the Appendix. The reasoning behind the selection of these standards include: the data shown from the XRF analysis, the soil composition literature, and the trial-and-error fitting of a number of other, unlisted reference compounds. Similar to that of bulk XANES, μ-XANES was also conducted utilizing the microcharacterization beamline (SXRMB) at the same photon-energy of 7200 eV. A pair of KB mirrors were used to focus the beam to a spot size of approximately 10 μm by 10 μm. Higher-resolution μ-XRF maps were generated through selecting areas based on the elemental distribution and correlation of specific

elements, such as P, Ca, and Fe. Once selected hotspots were acquired, a more localized μ-XANES spectrum was produced for each correlated location, similar to that of bulk XANES.

3.2.2 Nuclear Magnetic Resonance (NMR) Spectroscopy Analysis

Samples for NMR were extracted with NaOH-ethylenediaminetetraacetic acid (EDTA) in a modification of the Cade-Menun and Preston (1996) method for soils, using a sediment mass of 1.5 g and 25 mL extractant. The concentrations were determined by ICP analysis.

The freeze-dried sediment extracts were redissolved for P-NMR analysis with 0.6mL of D_2O, 0.6mL of H_2O, 0.6mL of the NaOH-EDTA extraction mixture, and 0.4mL of 10 M NaOH to keep the sample pH >13, mixed thoroughly with a vortex mixer (~10 min), centrifuged at 3260 rpm for 20 min to remove any solids, and then were transferred to NMR tubes (10-mm diameter). Samples were prepared and stored in the refrigerator (4ºC) for no more than 24 h prior to NMR analysis.

The ^{31}P-NMR spectroscopy was performed in the Saskatchewan Structural Sciences Centre (SSSC) at the University of Saskatchewan using a Bruker Avance 500-MHz spectrometer with a 45° pulse, 0.68 s acquisition time, 20 °C, 3.5s delay time, 1900-7400 scans (2.2-8.6 h), and no proton decoupling. The delay time was set at $4xT_1$ based on estimated T_1 values according to the ratio of P to Fe+Mn for each sample (McDowell et al., 2006). Peak identifications were based on the peak library of Cade-Menun (2015), and were confirmed with spiking experiments using *myo*-IHP, choline phosphate, α- and β-glycerophosphate, glyphosate and adenosine 5′ monophosphate, all purchased from Sigma-Aldrich. The full list of identified compounds can be found in Table A1, and a table of chemical shifts for identified peaks and example spectra are shown in Table A2, found in the appendix. Peak areas were calculated manually after integrating spectra processed with 7 Hz (full spectrum) and 2 Hz line broadening (orthophosphate monoester

and diester regions) using NUTS software (Acorn NMR, 2011 version). The results were corrected for diester degradation products by subtracting α- and β-glycerophosphate and the mononucleotides from the total monoester area and adding them to the total diester area (Young et al., 2013; Schneider et al., 2016). Peak areas in percentages were converted to concentrations for each sample (in µgP per g sediment) using the total P concentrations in each extract determined by ICP.

3.3 Statistics

For the XRF analysis, each sample was scanned once, though because the trends of elements were compared semi-quantitatively, instead of absolute values, it was considered to be acceptable. In terms of the XANES spectroscopy, each sample was scanned twice, and checked for reproducibility. Then, if acceptable, the average of these two nearly identical sets of data was then calculated and merged before being used for the final set of results. This of course applied to both the initial fingerprinting spectra, as well as the LCF analysis sections of the results. Though it is important to mention that the accuracy of LCF is potentially highly affected by the selection of references, baseline corrections and edge-step normalization procedures. The actual uncertainty associated with LCF has seldom been studied, with estimations of the associated error percentages ranging between 10%, 15%, and even as high as 17% (Gu, et al., 2019, Werner & Prietzel, 2015, Gustafsson, 2020). Consequently, a P fraction value smaller than 5% according to LCF analysis of XANES data is not considered to be reliable, and needs to be confirmed (Werner & Prietzel, 2015). All of these constraints support the need for simultaneous use of multiple methods in the study of P speciation.

For the NMR analysis, the samples were analyzed on a much larger scale than that of XANES analysis. The extracted samples are much larger in comparison and are thusly more representative of the whole sample material. Furthermore, thousands of scans were taken during each P-NMR experiment, ensuring precision of the results. Ideally, there would be duplicates of the samples analyzed in order to provide analytical variability, especially when considering that the major concern for this type of research is typically field study variability. However, accomplishing this is a great expense and is not entirely realistic.

4 Results and Discussion

The results and discussion from this research are separated into respective P K-edge XANES and P NMR sections. The samples analyzed in this project, as well as the techniques with which they were analyzed, are listed below in Table 4.1 below. The samples were collected from the Tintern Abbey (TTA), Ballynamona (BA), and Bunoke (BE) sampling sites, allowing the comparison of spatial influences, and to a certain degree, temporal influences on sediments. Moreover, these samples were also collected at different times throughout the year, allowing for proper comparison of the seasonality among samples. Finally, at both the Ballynamona and Bunoke sites, various samples were also collected from different catchment locations within the sites themselves, allowing comparisons between the inflow and outflow of the respective sampling sites.

Table 4.1: Sample List

Sample ID	
XANES	NMR
TTA-Sep17	TTA-Sep17
TTA-May18	TTA-Jun18
TTA-Jan18	TTA-Nov17
BA1-Jan19*	BE1-Jan19
BA1-Mar19	BE1-Mar19
BA1-Jun19	BE1-Jun19
BA2-Mar19	BE2-Jun19
BA3-Mar19	BE2-Mar19
BE1-Jan19*	BE3-Jun19
BE1-Mar19	BE3-Mar19
BE1-Jun19*	
BE2-Mar19	
BE2-Jun19	
BE3-Mar19	
BE3-Mar19	

*These samples have also been analyzed through μ-XANES

4.1 Molecular Characterization By XANES Spectroscopy

The XANES analysis results in this report are broadly separated into three general groups: XRF spectra, Bulk XANES spectra, and μ-XANES mapping/spectra of selected samples. The resulting XANES data are summarized and discussed both in terms of percentage and concentration.

4.1.1 X-Ray Fluorescence Spectra

The XRF spectra were generated at the CLS and normalized using Excel. The scattered X-rays, having an energy close to the incident photon energy, 7200 eV, and because they have a similar matrix, are assumed to have similar scattering efficiency. This then allows for the elemental distribution of each sample to be sufficiently shown and compared. The sample spectra for this section were separated by sample site, and the spectra for Tintern Abbey, Ballynamona, and Bunoke samples are displayed in Figures 4.1, 4.2, and 4.3, respectively:

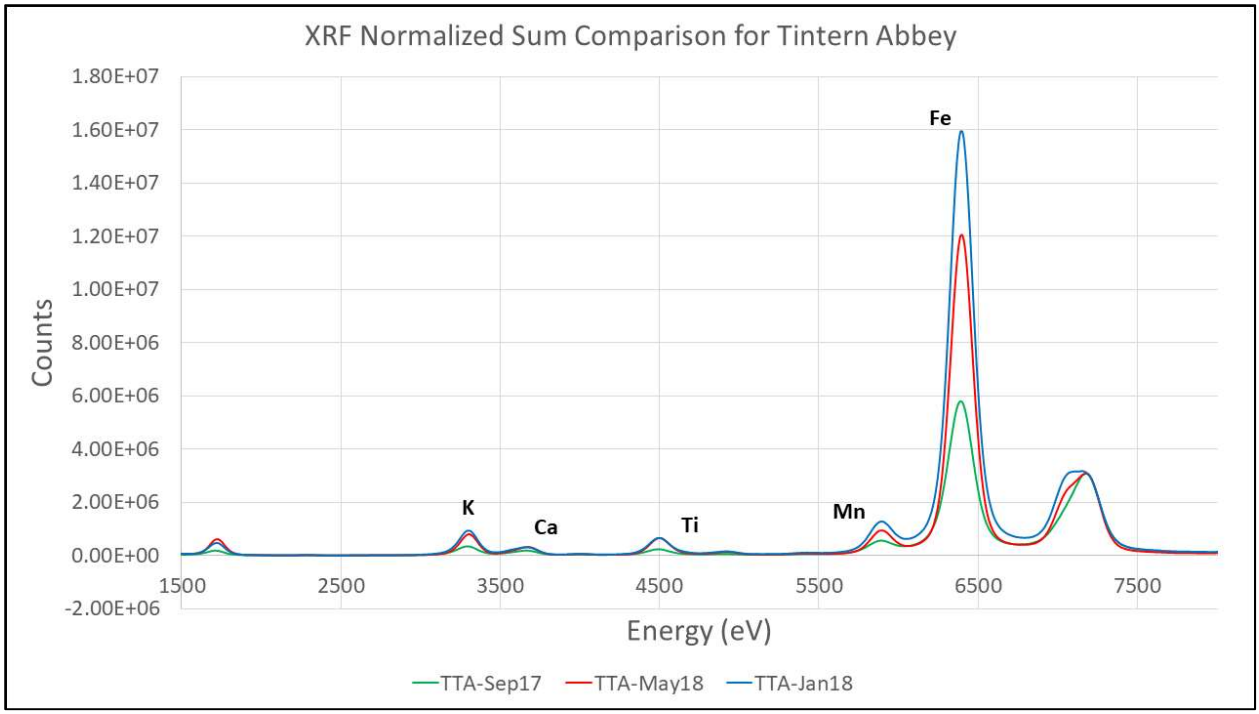

Figure 4.1: XRF Spectra for Tintern Abbey Site

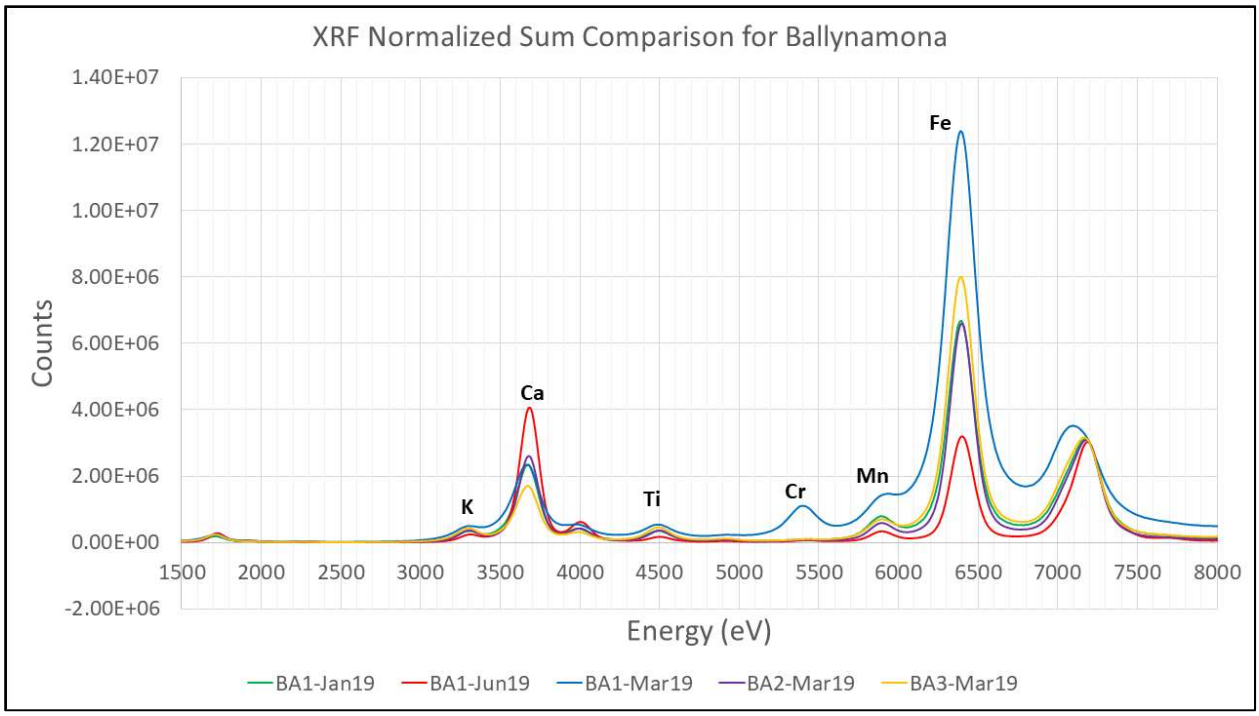

Figure 4.2: XRF Spectra for Ballynamona Site

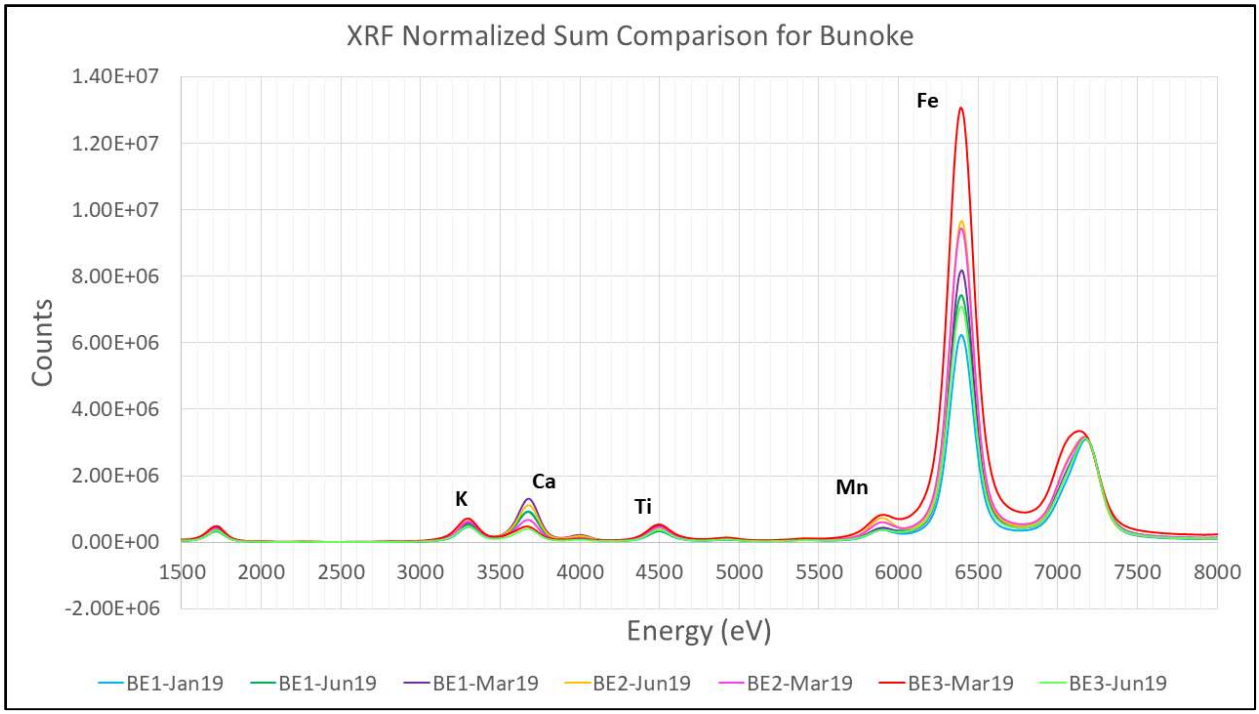

Figure 4.3: XRF Spectra for Bunoke Site

There are several important observations that can be made from these spectra. The first is that the samples tested show a wide variety of elemental distribution, not only among the sites and seasons, but also among the sampling locations within the sites themselves. Ballynamona for example, shows high Ca concentration relative to the other sites. This abundance can most likely be attributed to the soils and/or bedrock soil composition of the site, which contain a correspondingly high proportion of limestone and limestone bedrock, as well as highly alkaline water (Geological Survey of Ireland, 1998). Moreover, Tintern Abbey shows virtually no significant presence of potassium, which is more readily detected in the other sites. This may be because of the smaller environmental presence of volcanic rock, of which potassium is a major constituent, in the surrounding area when compared to that of Bunoke and Ballynamona. Curiously, BA1-Mar19 was found to have an uncharacteristically high amount of chromium, which seems most likely to be an anomaly. In any case, the results seen here indicated a spatial

influence on the elemental speciation of the sediment samples collected. However, all the samples tested appear to be largely dominated by Fe. This makes sense, as the samples are of sediment, which is known to typically contain a large amount of iron, in the form of mineral composition, particularly in clayey soils (EPA, 2003), as is the case with soils found at the sample sites used in this project.

The presence of Fe varied greatly depending on the time of year that the sample was taken. The precipitation data corresponding to the different sites, which can be seen in Table 3.1 and Figure 3.4, show a steady and significant difference in the amount of rainfall seasonally, with less Fe consistently in sediments collected in the drier months of June and September. This may be because the increased rainfall agitates the riverbed and increases the geological contribution of the environment itself to the sediment. In other words, there is less soil runoff in the drier months. Moreover, the climate data also shows a clear difference in the seasonality between the sites of Ballynamona/Bunoke, and that of Tintern Abbey, which regularly sees lower rainfall during the sampling times. However, this difference can more clearly be seen in the XANES spectra shown later in the thesis. This project, outside the scope of this report, has already shown that mineral linked P compounds have a significant effect on the transformation and cycling of P in fluvial systems (Zhang, 2020).

Finally, while XRF shows quite a bit of activity and information regarding other elements, it is also worth noting that P concentrations were relatively low in all of the samples tested, further implying the need for more advanced molecular characterization techniques, such as XANES or NMR spectroscopy, to be discussed below. Furthermore, even a relatively small amount of P can have a major impact on both the eutrophication and the water quality of the respective aquatic system, if P is the nutrient limiting algal/bacterial growth.

4.1.2 Bulk XANES Data

For the XANES analysis, every sample in this section was analyzed with bulk XANES, detailed below. Selected samples were also analyzed with μ-XANES, detailed in a separate section.

4.1.2.1 XANES Bulk Spectra

The XANES spectroscopic analysis was performed at the CLS for each sample in this section, and the spectra generated were normalized using Athena software, (Ravel & Newville, 2005). These data were then truncated and overlaid to differentiate results and sort the samples based on the different sites involved. The bulk XANES spectra for Tintern Abbey, Ballynamona, and Bunoke sites are displayed in Figures 4.4, 4.5, and 4.6 below.

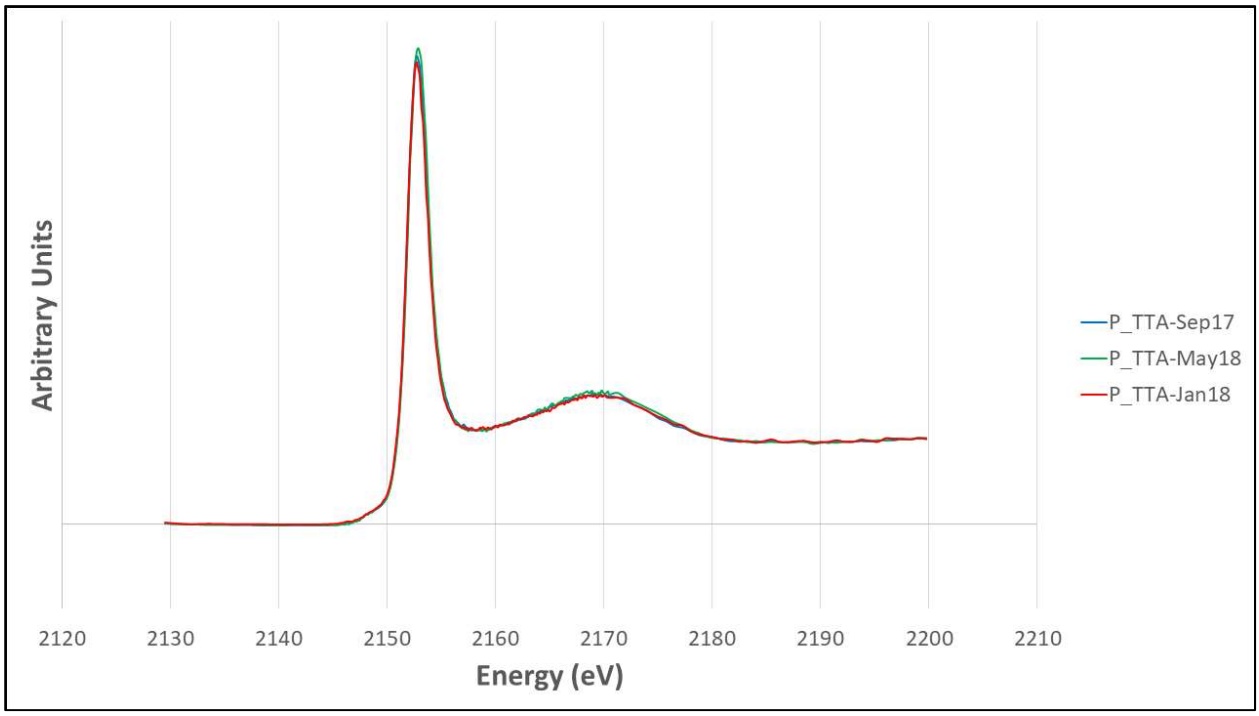

Figure 4.4: Bulk XANES K-Edge Spectra for P in Tintern Abbey (TTA)

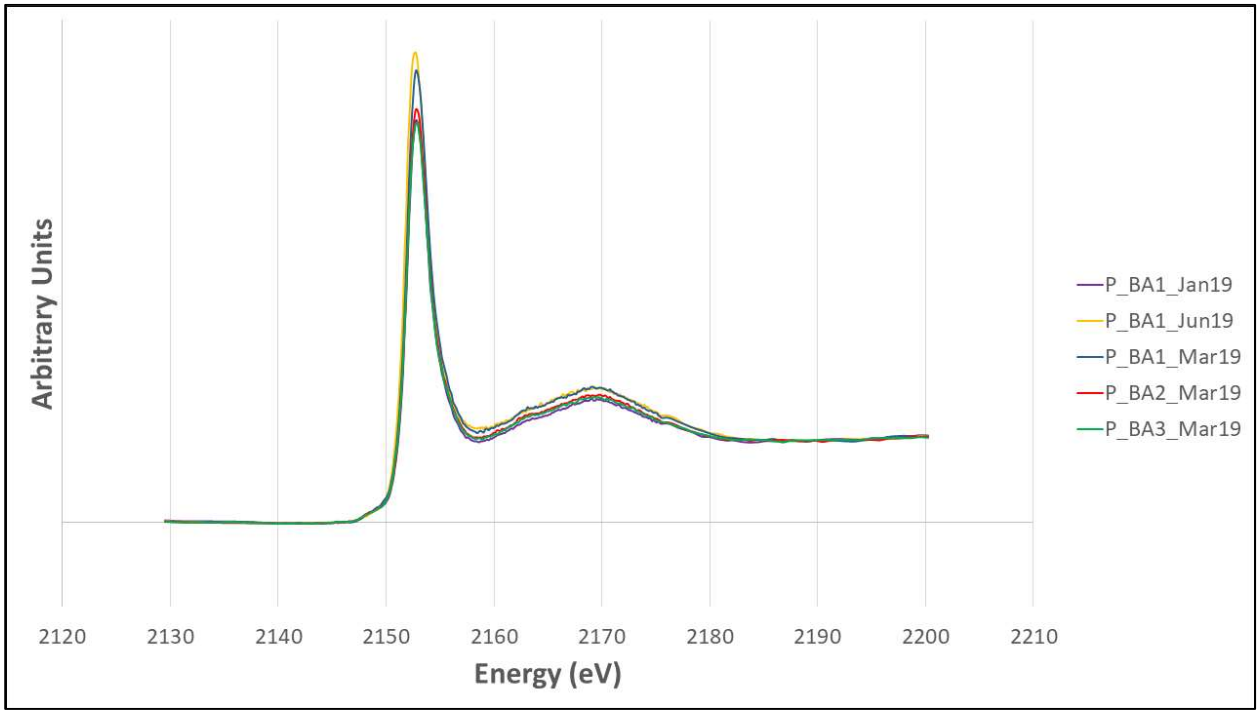

Figure 4.5: Bulk XANES K-Edge Spectra for P in Ballynamona (BA)

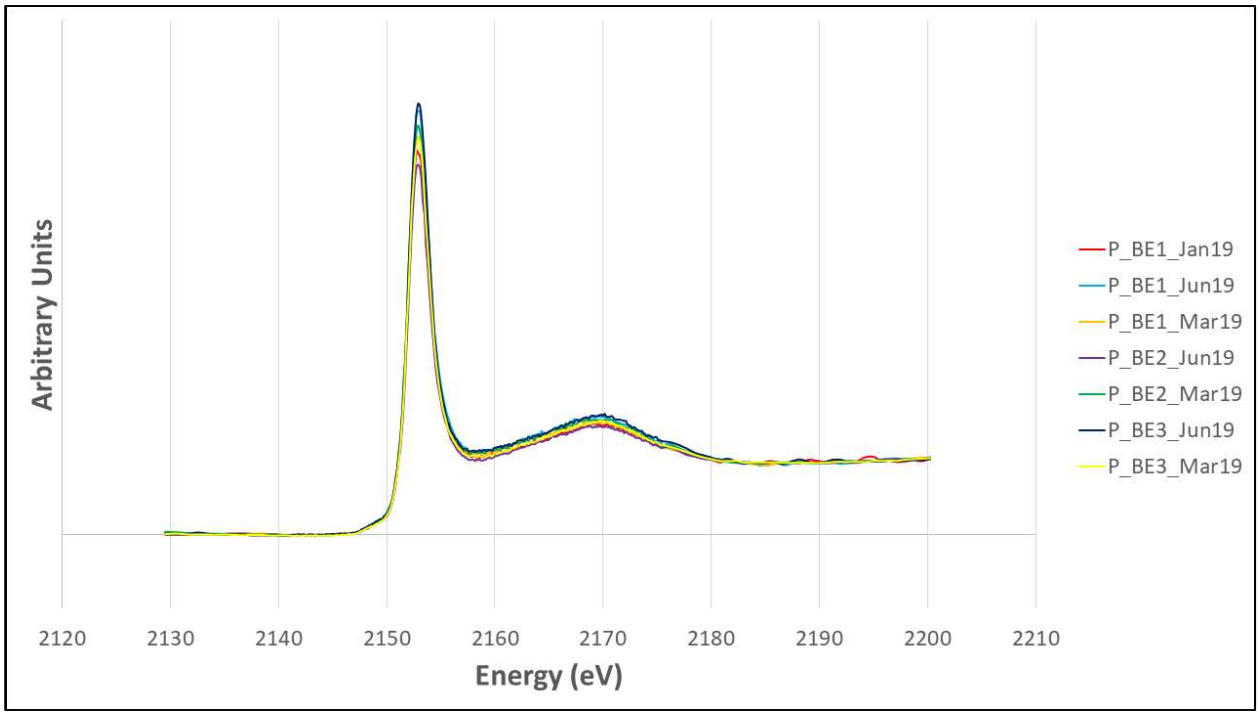

Figure 4.6: Bulk XANES K-Edge Spectra for P in Bunoke (BE)

4.1.2.2 LCF Distribution Data

From the initial bulk spectra, what is known as fingerprinting analysis was performed, wherein the peaks and shape of the produced spectra were visually identified as more specific compounds and elements. This serves, among other purposes, as a helpful guide towards linear combination fit (LCF) analysis. The reference standards, and their respective spectra, used for comparison of bulk XANES analysis, as well as for the LCF analysis, can be found in the Appendix. The LCF analysis was performed within the same program (Ravel & Newville, 2005) and the fitted spectrum was generated for each sample individually, which can be referenced in this thesis in the Appendix. A summary of the quantitative distribution for each of the samples is listed in Tables 4.2 and 4.3 below, along with the relevant reference standards, both in terms of percentage of the total sample and in concentration. The reference standards used to represent the inorganic P compounds, namely $FePO_4 \bullet 2H_2O \bullet Si$ and $Ca_3O_3P_3 \bullet Si_3$, are consistent for each sample, while the organic standard is based on sorbed phytate.

Table 4.2: LCF Distribution Results Summary in Percentage (%)

Sample ID	Fe-P	Ca-P	Organic-P	Organic Standard
TTA-Sep17	0.381	0.206	0.413	Phytic Acid (Ca)
TTA-May18	0.456	0.190	0.354	Phytic Acid (Ca)
TTA-Jan18	0.331	0.234	0.435	Phytic Acid (Ca)
BA1-Jan19	0.399	0.540	0.062	Phytic Acid (Si)
BA1-Mar19	0.433	0.287	0.281	Phytic Acid (Ca)
BA1-Jun19	0.326	0.000	0.674	Phytic Acid (Si)
BA2-Mar19	0.420	0.475	0.123	Phytic Acid (Si)
BA3-Mar19	0.395	0.519	0.086	Phytic Acid (Si)
BE1-Jan19	0.443	0.281	0.276	Phytic Acid (Si)
BE1-Mar19	0.488	0.189	0.322	Phytic Acid (Si)
BE1-Jun19	0.523	0.191	0.285	Phytic Acid (Ca)
BE2-Mar19	0.488	0.142	0.371	Phytic Acid (Ca)
BE2-Jun19	0.443	0.422	0.134	Phytic Acid (Si)
BE3-Mar19	0.490	0.249	0.261	Phytic Acid (Si)
BE3-Jun19	0.577	0.031	0.392	Phytic Acid (Si)

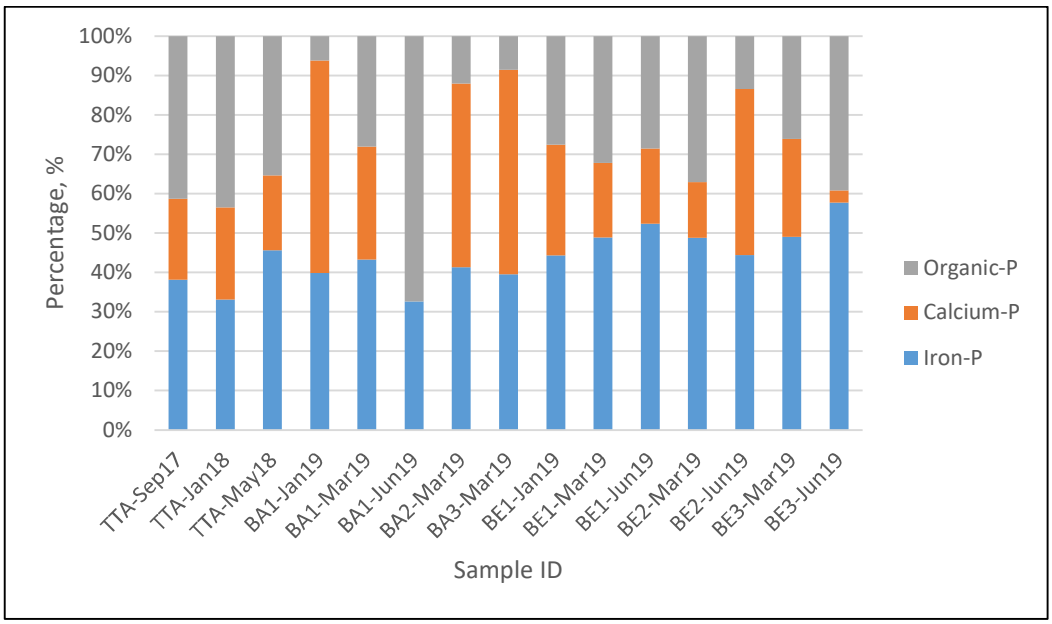

Figure 4.7: LCF Distribution Results Stacked Bar Total Summary Percentage (%)

Table 4.3: LCF Distribution Results Summary in Concentration (µg g^{-1})

Sample ID	TP (µg g^{-1})	Fe-P (µg g^{-1})	Ca-P (µg g^{-1})	Phytate (µg g^{-1})	Phytate Standard
TTA-Sep17	332.4	126.6	68.5	137.3	Phytic Acid (Ca)
TTA-Feb18	1657.7	398.8	281.9	524.1	Phytic Acid (Ca)
TTA-Jun18	1204.8	755.9	315.0	586.8	Phytic Acid (Ca)
BA1-Jan19	2413.6	963.0	1303.4	149.6	Phytic Acid (Si)
BA1-Mar19	4528.8	1961.0	1299.8	1272.6	Phytic Acid (Ca)
BA1-Jun19	2736.5	892.1	0.0	1844.4	Phytic Acid (Si)
BA2-Mar19	10628.6	4464.0	5048.6	1307.3	Phytic Acid (Si)
BA3-Mar19	11493.4	4539.9	5965.1	988.4	Phytic Acid (Si)
BE1-Jan19	1304.7	578.0	366.6	360.1	Phytic Acid (Si)
BE1-Mar19	1296.1	632.5	245.0	417.4	Phytic Acid (Si)
BE1-Jun19	2749.7	1438.1	525.2	783.7	Phytic Acid (Ca)
BE2-Mar19	2978.4	1453.5	422.9	1105.0	Phytic Acid (Ca)
BE2-Jun19	2829.8	1253.6	1194.2	379.2	Phytic Acid (Si)
BE3-Mar19	2805.7	1374.8	698.6	732.3	Phytic Acid (Si)
BE3-Jun19	2438.8	1407.2	75.6	956.0	Phytic Acid (Si)

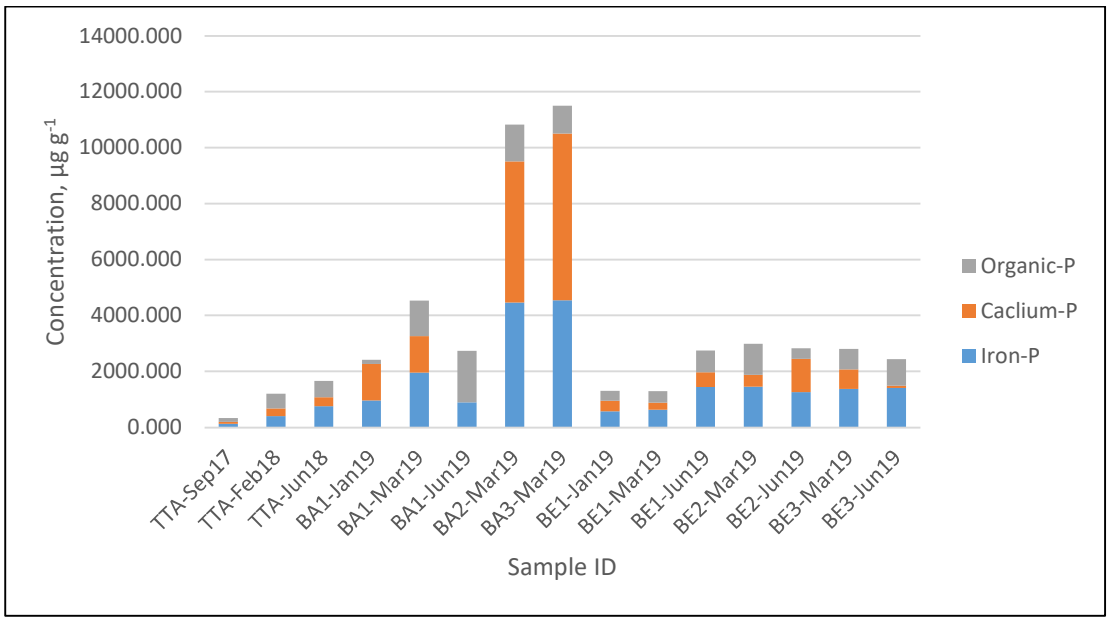

Figure 4.8: LCF Distribution Results Stacked Bar Total Summary Concentration (µg/g)

XANES is an extremely useful tool to study the speciation of a sample, as it can show, with relatively high detail, the different molecular compounds linked to P in the sample. Several observations can be made about the results obtained through XANES analysis, both through the bulk spectra and the LCF distribution. The first is that the bulk XANES spectra have shown the samples analyzed to be fairly similar to one another. That, alongside the mostly symmetrical and narrow nature of the resulting spectra, suggest that the samples are largely inorganic in concentration, in regards to P speciation. It can also be observed that the samples spectra from Ballynamona seem to show a presence of calcium-linked phosphate, which was also observed to contain higher amount of Ca in the XRF data discussed earlier, showing the same increased presence and further supporting the importance of the techniques. Finally, there was a weak, pre-shoulder on the spectrum for each site, indicating iron associated P. Again, this was also found in the XRF distributions, highlighting the importance of the techniques when used alongside one another.

When looking at the LCF distribution results, perhaps the most apparent observation is that a lot of variations can be seen among the sites, the sampling periods, and the locations within the sites. Though there are inconsistencies, the general trend of a relatively larger presence of Fe-linked P in the drier months can be observed in the LCF results. This is particularly interesting when considering that the XRF data showed the opposite trend with respect to Fe concentration. This would then imply that the lower Fe concentrations found in drier months may be relatively highly associated with P compounds, or the higher amount of Fe in wetter months is not necessary all related to Fe-P.. This relationship may also be attributed to increased farming activities during the summer months, or even perhaps the higher associated temperatures seen during this period, which would, in turn, then allow for more interaction between FeO_x and

organic, or dissolved P, and thusly an increased presence of Fe-P. Though the effects of Fe oxides on the relevant measured P forms have been shown to vary from study to study, though the inorganic P has commonly been found to be positively correlated with crystalline iron oxide content (Shiau, 2018), which is a relationship that can also be observed in the results from this research as well.

Both the percentage distribution as well as the corresponding concentrations, show that samples collected during the wetter months of February or March contain less organic P, when compared to samples from the drier months. This may be due to an increase in the amount of P loading correlated to the increase in higher precipitation, and by extension the soil agitation. More rainfall means that the there will be less trapped particles in the sediments. The same observations made when analyzing the bulk XANES spectra are shown more quantitatively in the LCF data. This includes the confirmation of a significant presence of Ca-linked P in the BA samples. Ballynamona, when compared to the other sites, has more calcareous parent material and alluvium, implying a contribution of soil composition to the P characterization. Perhaps most surprising from the LCF distribution is the variability among sampling locations within the same sites. The different sample locations differ only slightly in geology, despite showing a relatively large amount of variance in characterization. That being said, the correlation observed between inflow and outflow catchments for, Bunoke and Ballynamona, shows the opposite effect on speciation. More work on source tracing is needed for a better understanding on the spatial influences.

Another important observation is that the LCF fitting produced reasonably closely-fit, if not perfect, results. By visual inspection, one can immediately see that the pre-edge peak at around 2149 eV, corresponding to Fe-P, is relatively overestimated by the LCF fitted spectra. The same

can be observed regarding the post-edge 'shoulder' of Ca-linked P, at around 2155 eV. Therefore, one could argue that the sorbed organic P is perhaps under-fitted. This proves to be consistent throughout all of the samples, though it can best be seen in Figure 4.9 below. The remaining sample spectra can be found in the Appendix. From these spectra, it seems fair to claim that the LCF distribution overly favors inorganic P, which agrees with the initial inspection mentioned earlier. Finally, it is worth mentioning that the fitting error of LCF analysis is typically 5-10%, which may account for part of difference (Zhang, 2020, Werner & Prietzel, 2015).

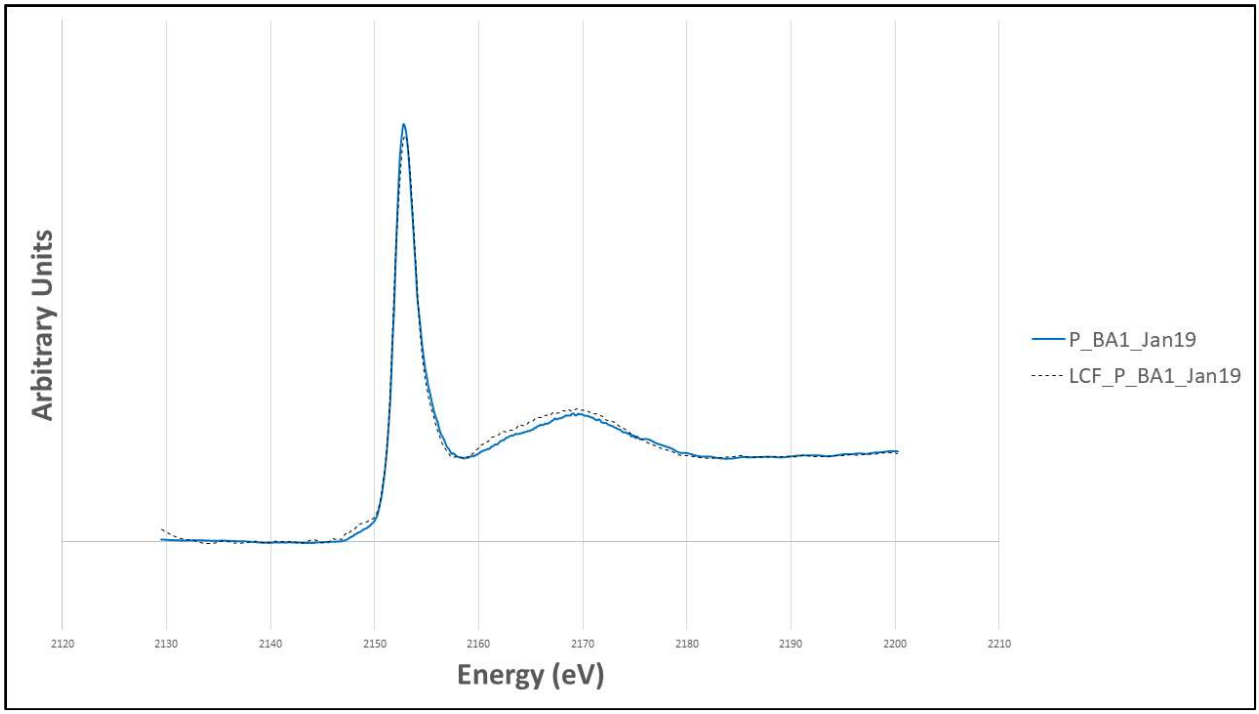

Figure 4.9: Example of LCF fitting spectrum (BA1-Jan19)

P K-edge XANES analysis, while extremely useful, is limited with respect to the identification of organic P compounds, which in turn demonstrates the need for NMR spectroscopy alongside XANES analysis. This technique will be necessary in order to understand the full

characterization, as it can detect organic P molecular compounds that XANES spectroscopy cannot. Moreover, a comparison of the results obtained in this section and those obtained through NMR analysis is included in section 4.3.

4.1.3 μ-XANES Spectra

As mentioned before, μ-XANES can be an extremely useful tool when looking to better understand the comprehensive picture of a sample. This is particularly useful when determining the localized speciation within a sample, and can show which metal molecular associations are linked to P, and where in the sample these relationships can be found. In order to obtain the μ-XANES data, XRF mapping images were first generated for each of the samples analyzed. These images were then inspected to locate areas of interest known as 'hotspots', shown in the figures below as sp1 and sp2. These locations were then analyzed in order to generate more detailed and focused spectra. These spectra can demonstrate differences in elemental presence and molecular characterization within samples when compared to the initial bulk XANES analysis. The initial XRF mapping image gives an idea of relevant hotspots for further analysis. The preliminary mapping images, as well as their corresponding spectra provided by Athena, are depicted in figures below.

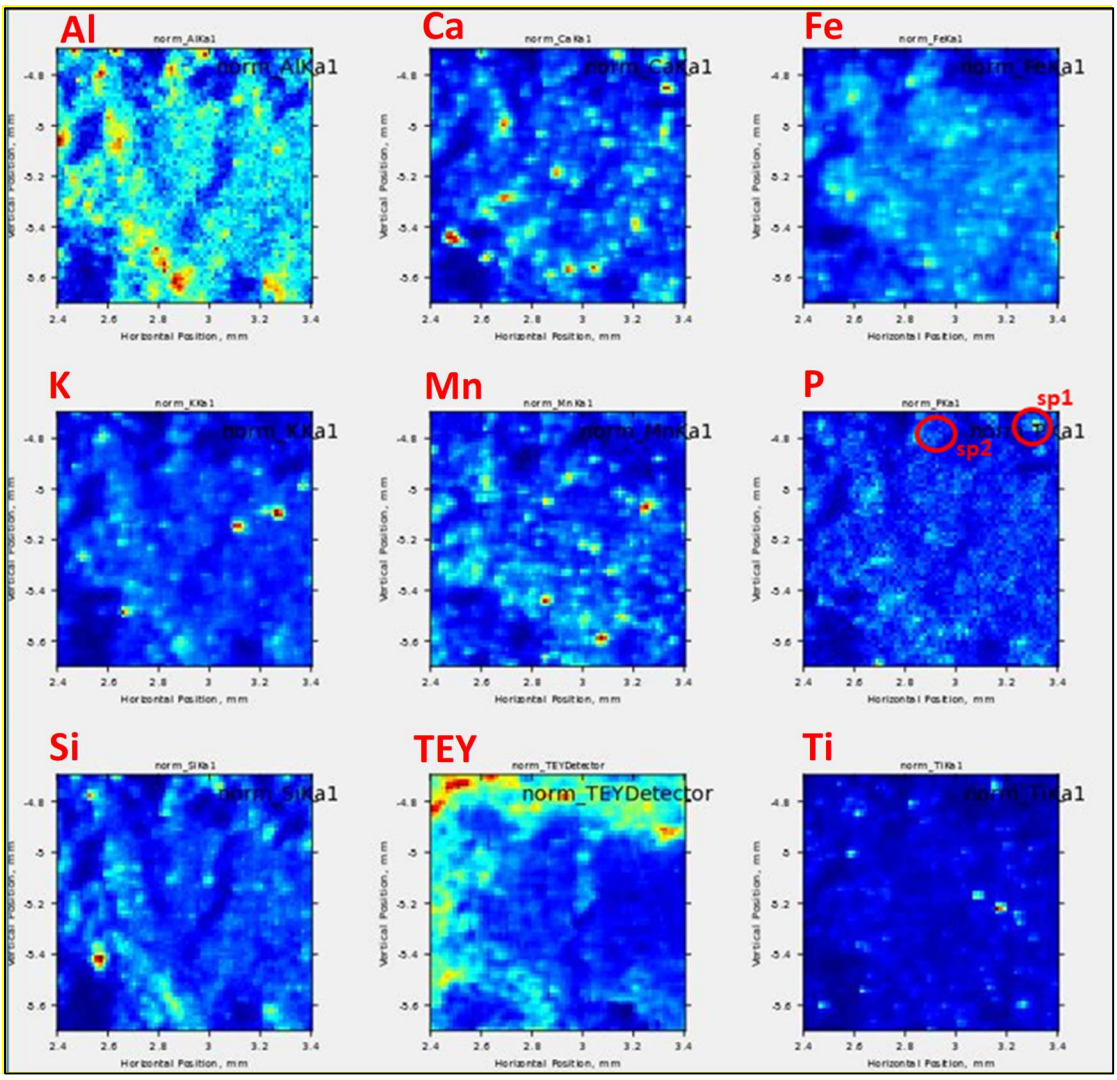

Figure 4.10: μ-XANES Associated Elemental Mapping Image for BA1-Jan19 (Concentration goes from maximum to minimum when color goes from red to blue)

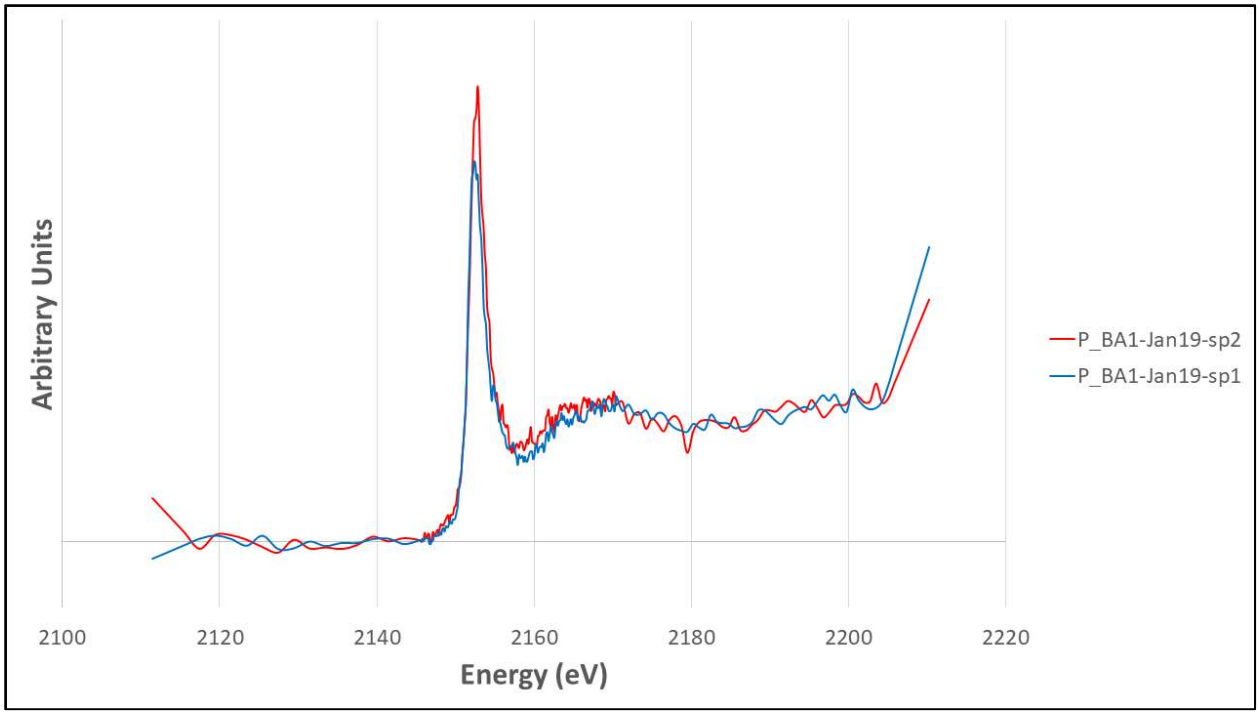

Figure 4.11: μ-XANES K-Edge Spectra for BA1-Jan19

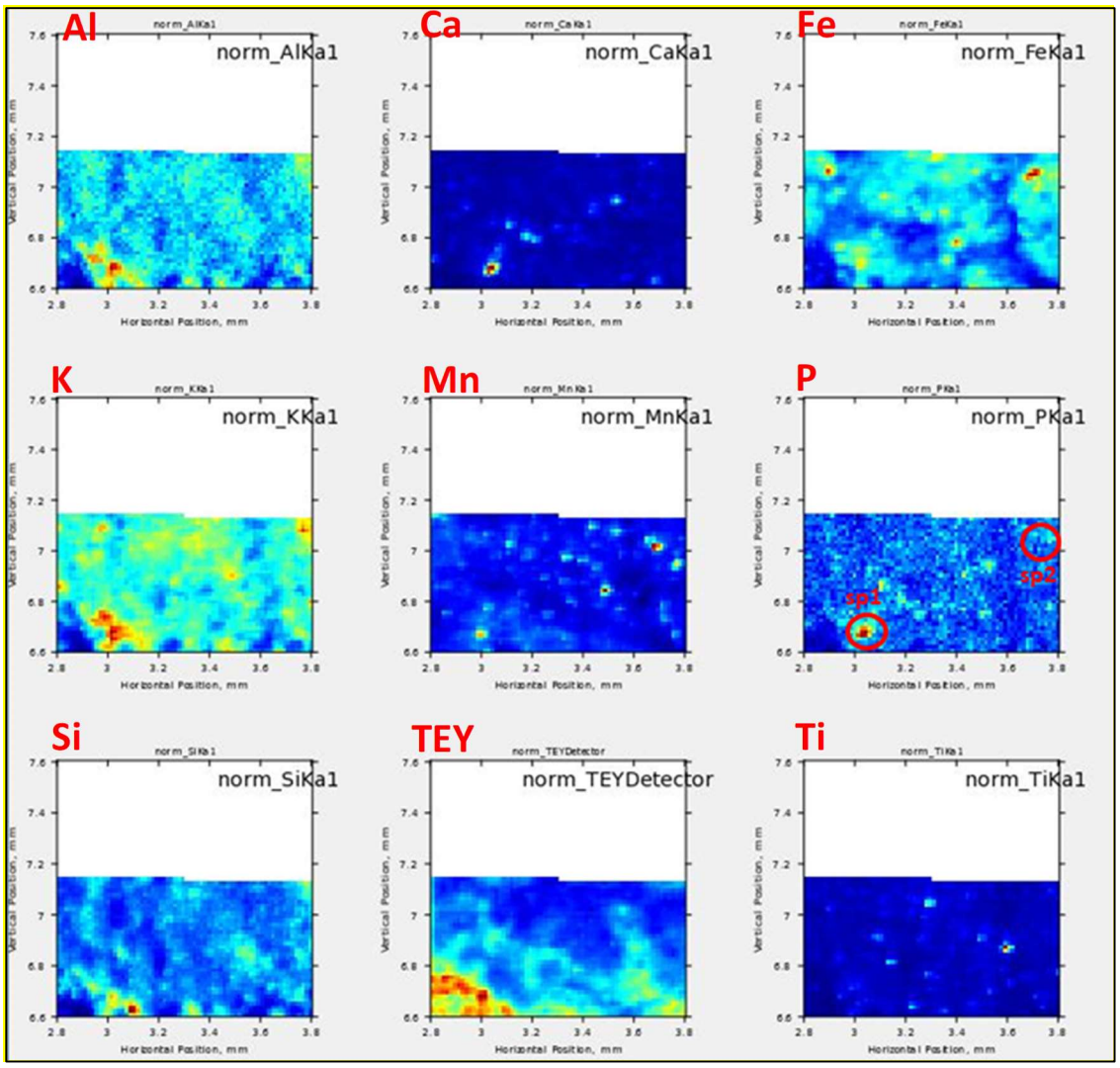

Figure 4.12: μ-XANES Associated Elemental Mapping Image for BE1-Jan19 (Concentration goes from maximum to minimum when color goes from red to blue)

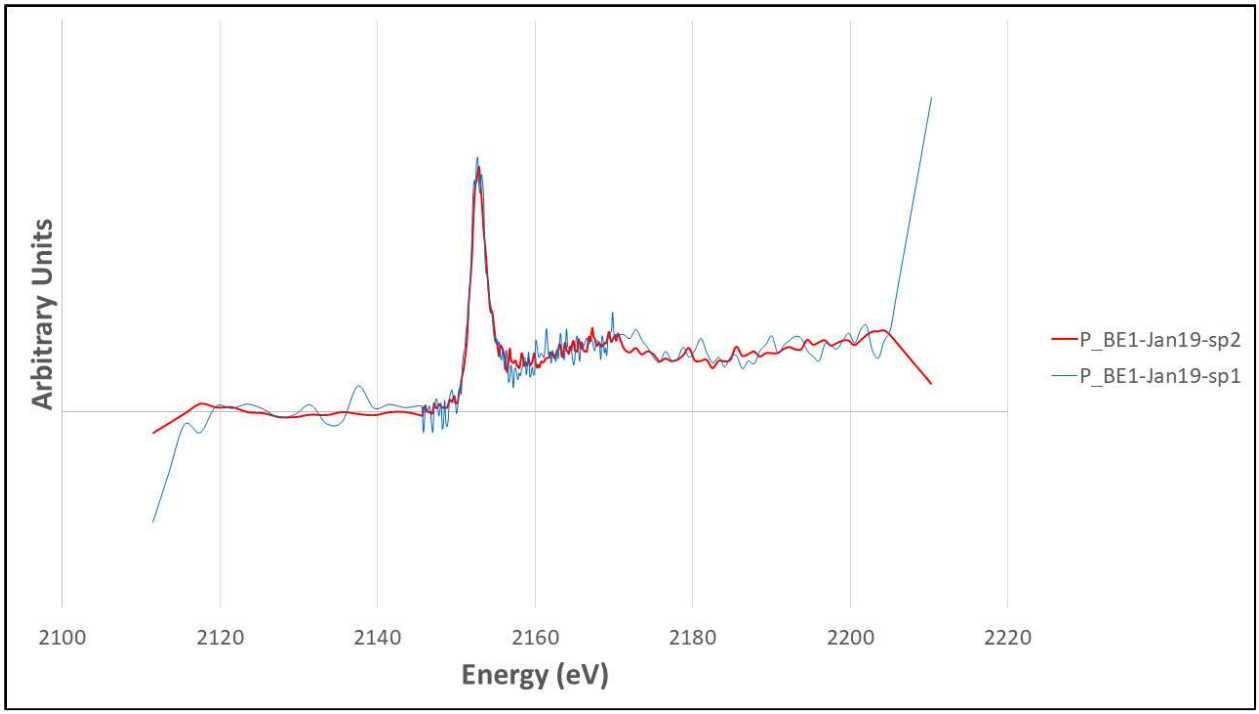

Figure 4.13: μ-XANES K-Edge Spectra for BE1-Jan19

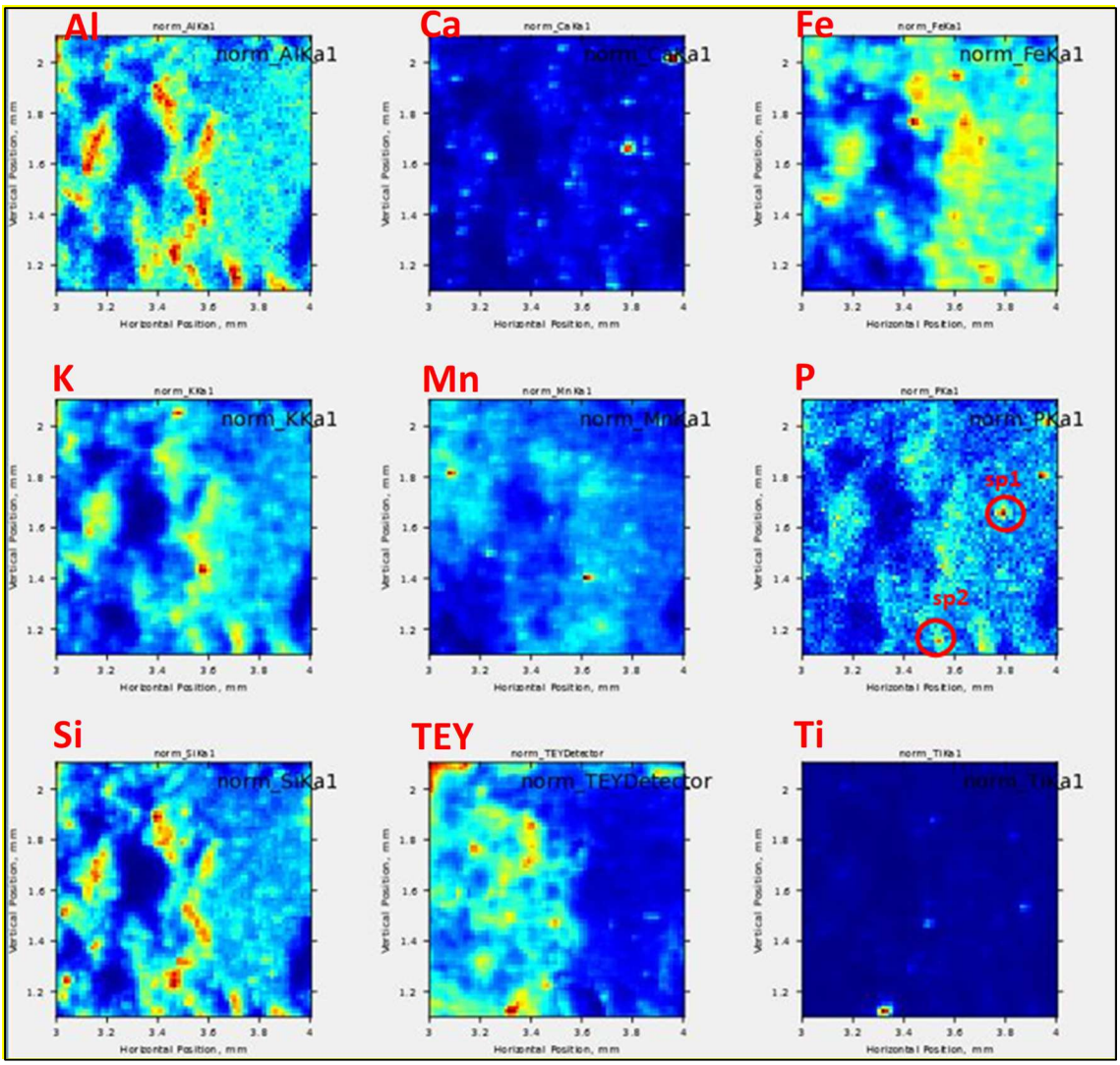

Figure 4.14: μ-XANES Associated Elemental Mapping Image for BE1-Jun19 (Concentration goes from maximum to minimum when color goes from red to blue)

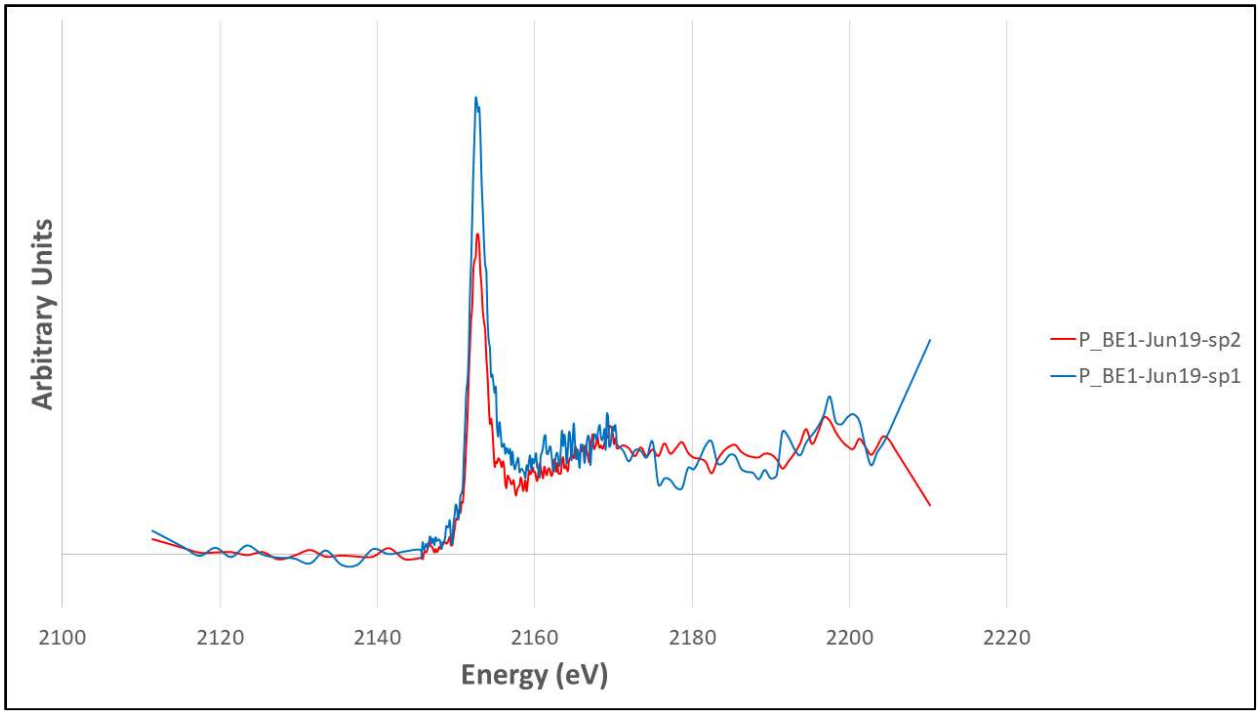

Figure 4.15: μ-XANES K-Edge Spectra for BE1-Jun19

There are a couple of important conclusions that can be drawn from the μ-XANES analysis results. First and most importantly, the diversity shown between each of the three different samples analyzed demonstrates how μ-XANES can be uniquely beneficial to understand the full speciation of a sample.

Each sample shows a different degree of variability from the original bulk spectra. The first sample analyzed, BA1-Jan19, showed possible correlations between Ca and P in the initial mapping, as noted by the two marked hotspots, shown in Fig 4.10. The sample was then further analyzed to generate the μ-XANES spectra, shown in Fig 4.11, which showed the 'post-edge shoulder' indication of calcium, seen as an upwards trend in the spectra at around 2160 eV, supporting what was predicted from the mapping. There was an issue with the motor during the mapping of the second μ-XANES sample listed, BE1-Jan19, that prevented the full image from

being shown, seen in Fig 4.12. However, important correlations were still able to be seen, such as the possible relationship between that of P and calcium, displayed in Fig 4.13. When further analyzed, the spectra of the sample showed little indication of calcium, meaning the correlated calcium observed in the initial mapping may not be linked to P. Finally, the third sample, BE1-Jun19, showed a homogeneous spread of P throughout the sample, with possible elemental correlations of calcium, iron, and potassium (Fig 4.14). When analyzing the sample further, XANES spectra showed a difference between the hotspots selected, with 'hotspot 1' showing the Ca and Fe predicted by that of the initial XRF mapping.

More broadly speaking, these samples, and section, demonstrate the usefulness of μ-XANES analysis as a powerful tool of P characterization. This technique, as demonstrated by the included examples, allows for the closer inspection of samples, and molecular interactions that would otherwise remain unseen. In the context of this study, BA1-Jan19 was found to be relatively homogeneous in its P concentration, shown to be fairly spread out throughout the sample area, while BA1-Jun19 and BE1-Jun19 were found to be much more heterogeneous, exhibiting distinct areas of concentrated P. When comparing μ-XANES with that of bulk XANES, one can note the usefulness of using both congruently alongside one another, as compounds displayed by one can be supported or contrasted by the other, such as the case with Ca-P compounds.

4.2 Molecular Characterization Through Use of ^{31}P-NMR Spectroscopy

The NMR spectroscopic analysis are presented as figures showing the collected spectra, and in tables showing the calculated concentrations of general P compound classes and specifically identified P compounds. Unfortunately, some of the samples taken do not directly correlate to the

sampling periods seen in the XANES analysis section, but these are the closest relationships that can be used and significant comparisons can still be made. This experiment includes samples taken from various sites and different seasonal periods.

The spectral data can be found summarized in the figures below. Figure 4.16 displays spectra for samples from the Tintern Abbey sampling site, and Figure 4.17 shows the corresponding monoester region, while Figure 4.18 shows spectra for samples from the Bunoke site, and Figure 4.19 shows the corresponding monoester region. In both, spectra are plotted with 7 Hz line-broadening and scaled to the height of the orthophosphate peak in each spectrum.

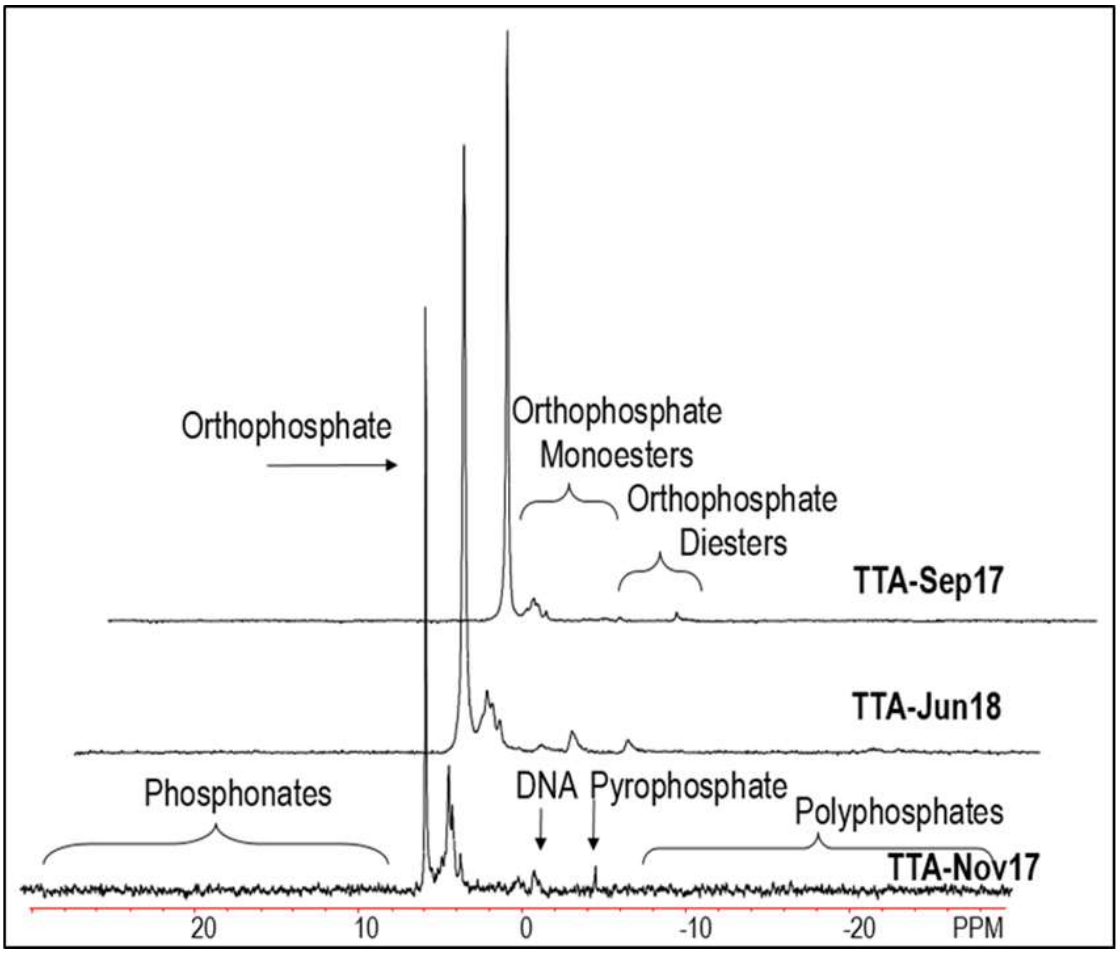

Figure 4.16: ^{31}P NMR spectra for samples from Tintern Abbey, processed with 7 Hz line broadening and scaled to the height of the orthophosphate peak in each spectrum.

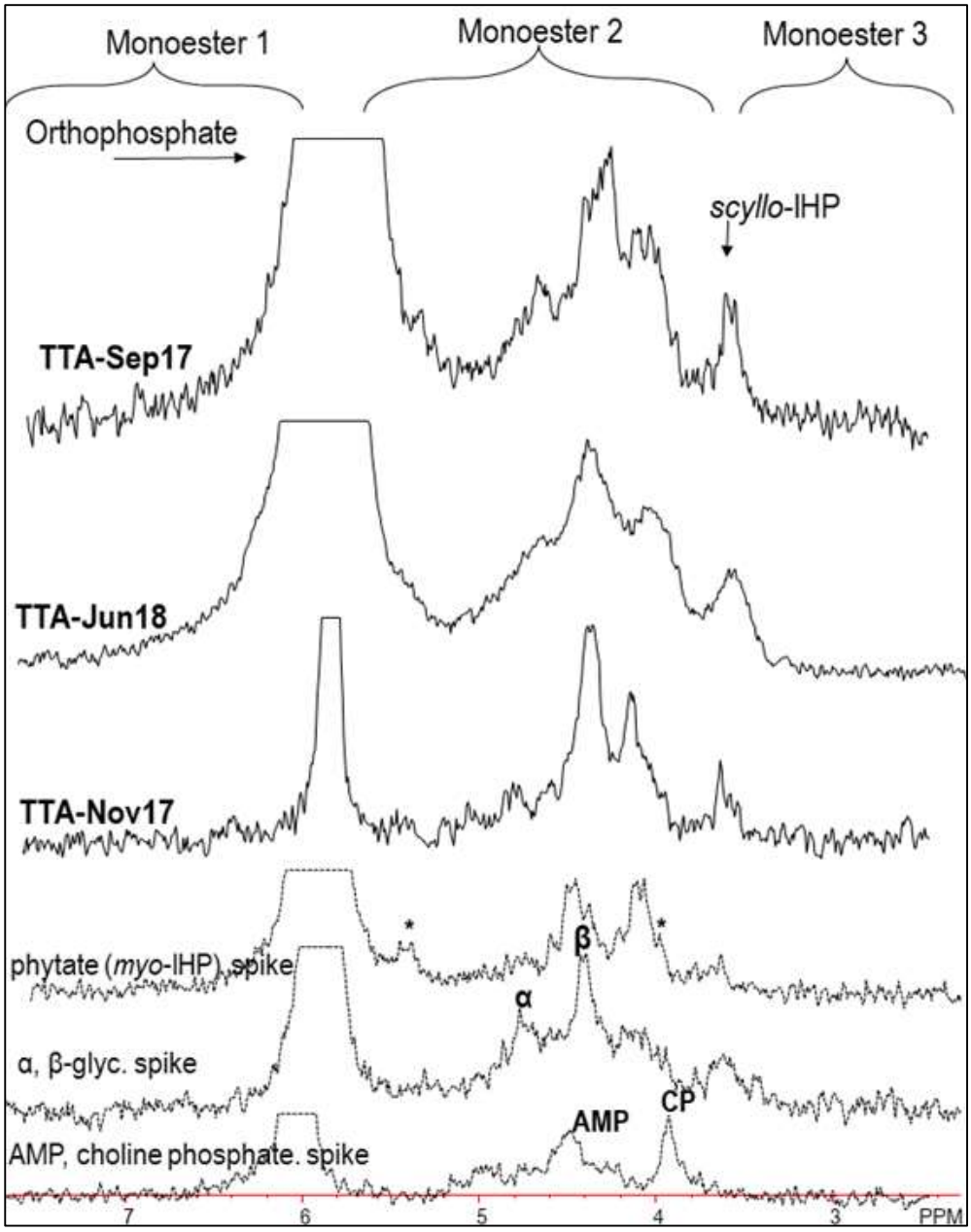

Figure 4.17: Enhanced monoester regions for the ^{31}P NMR spectra corresponding to the samples from Tintern Abbey, processed with 7 Hz line broadening and scaled to the height of the orthophosphate peak in each spectrum.

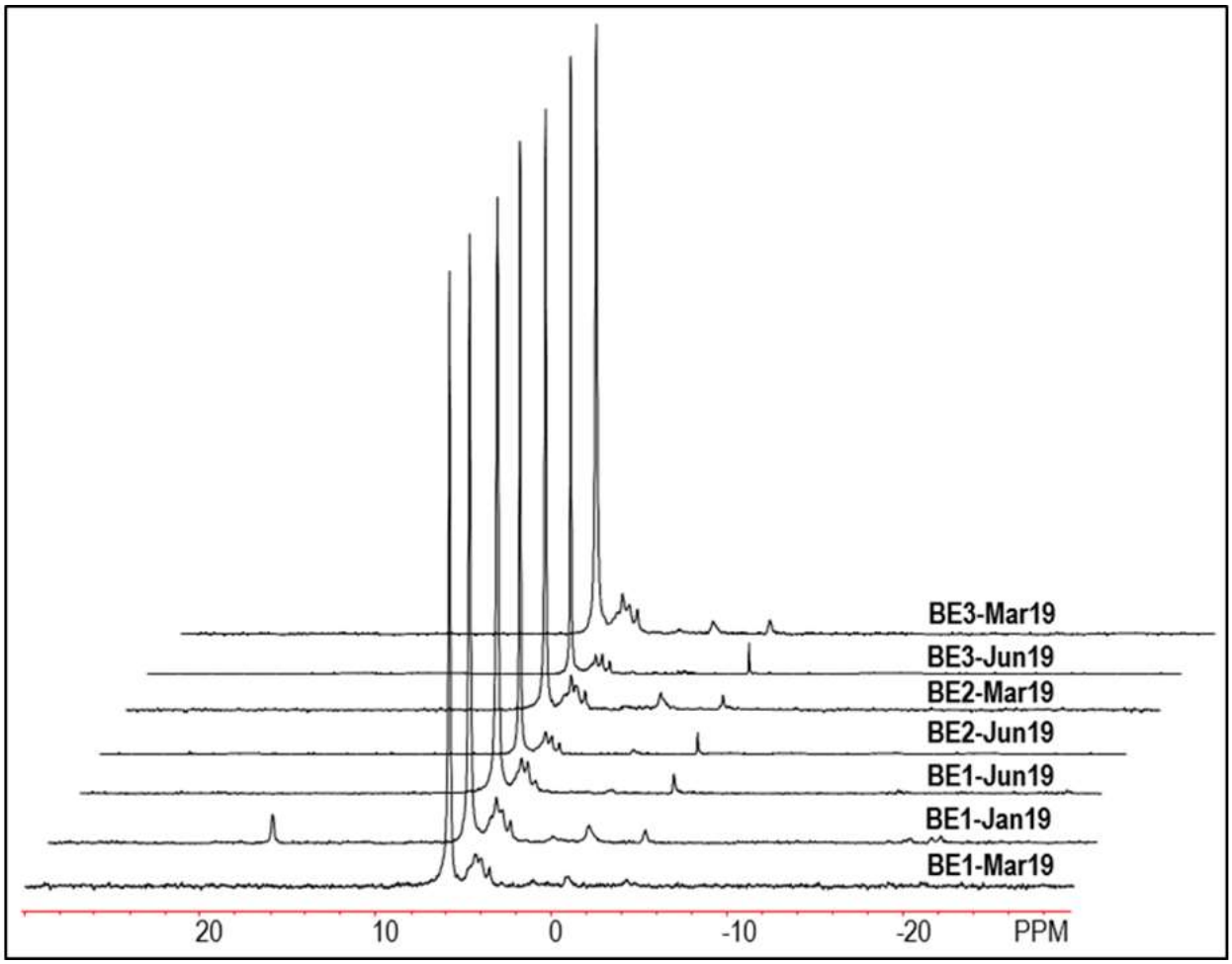

Figure 4.18: ^{31}P NMR spectra for samples from Bunoke, processed with 7 Hz line broadening and scaled to the height of the orthophosphate peak in each spectrum

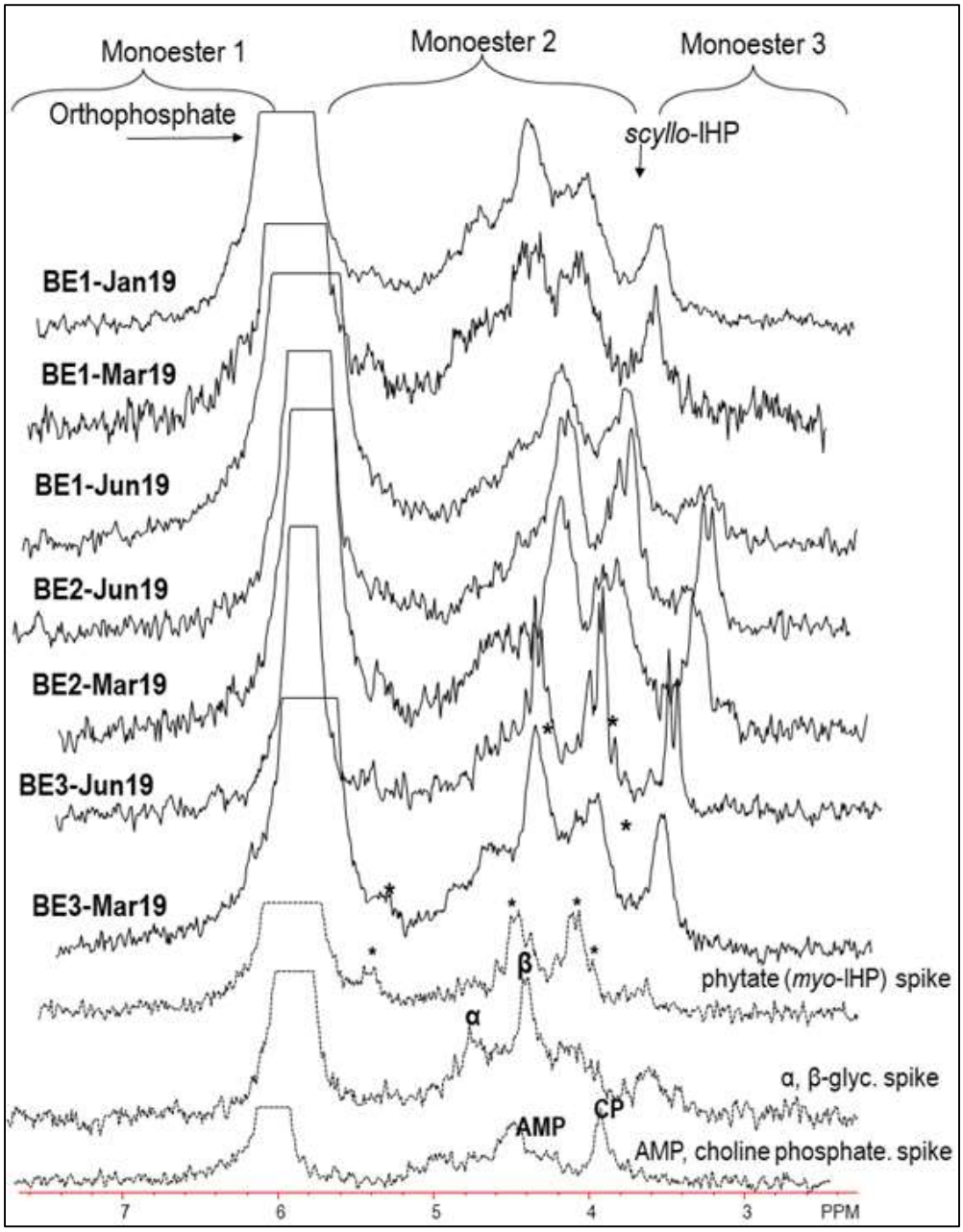

Figure 4.19: Enhanced monoester regions for the ^{31}P NMR spectra corresponding to the samples from Bunoke, processed with 7 Hz line broadening and scaled to the height of the orthophosphate peak in each spectrum.

There are a couple of initial observations that can be made regarding the generated NMR spectra. The first observation is that there is a range in spectral resolution between the samples. This is most likely attributed to the differences in concentrations, with some of the noisier samples, such as TTA-Nov17, having less P and more Fe and Mn. The issue of line broadening can be addressed, to some extent, by dilution of the sample, but there is an associated concern of falling below the detection limit when diluting samples with already low P concentration.

Upon initial visual inspection, several important P forms and compound classes can be immediately identified, such as orthophosphate and peaks in the orthophosphate monoester and orthophosphate diester regions. Forms of P in much lower concentrations can also be identified, though it is considerably easier to see through the tabulated data.

Concentrations of P compounds and general compounds classes are displayed in the tables below. Table A1 shows the total results for specific compounds, found in the Appendix, while Table 4.4 shows the calculated data organized into more general compound categories. These results were determined by calculating the areas for each peak with the integration routine in the NMR software, and then multiplying peak areas by the P concentration in the extract for each sample. Moreover, the chemical shifts used for each sample are displayed in Table A2 found in the Appendix.

Table 4.4: ^{31}P NMR Results Simplified Summary (μg/g)

Sample ID	%Rec*	Pi	Po	TotPoly	TotPhn	TotIHP	myo:other	Cmono	Cdiest	Deg	cM:D
TTA-Sep17	95.5	242.4	74.9	10.8	2.2	19.0	0.76	45.1	27.6	14.6	1.63
TTA-Nov17	16.9	101.8	150.9	8.6	3.5	27.3	0.50	60.7	86.7	57.1	0.70
TTA-Jun18	12.5	131.8	75.8	11.4	1.5	12.9	0.68	37.6	36.7	18.3	1.02
BE1-Jan19	12.5	99.5	63.6	9.1	2.4	9.8	0.67	27.6	29.2	16.8	0.94
BE1-Mar19	22.4	190.2	100.2	16.0	4.1	21.5	1.00	56.3	39.8	21.8	1.42
BE1-Jun19	85.2	1678.9	662.7	86.6	16.4	189.7	1.25	395.7	250.6	180.3	1.58
BE2-Mar19	32.2	590.3	368.0	49.8	13.4	80.5	1.00	166.7	187.8	73.8	0.89
BE2-Jun19	61.6	1267.1	475.8	76.7	26.1	141.2	1.25	282.4	167.3	102.8	1.69
BE3-Mar19	30.3	561.9	288.2	31.5	12.8	59.5	0.67	153.9	121.6	64.6	1.27
BE3-Jun19	78.0	1331.6	570.7	98.9	13.3	184.5	0.73	315.8	241.6	142.7	1.31

*%Rec represents the percentage of P recovered in the NaOH extract; Other pools can be identified in the chemical shifts table (Table A2)

There are several important observations that can be made about the NMR results. The variation seen within the results from the XRF and XANES analysis can be observed here as well, with a variety of different P compounds visible in both the spectra and the calculated data. There were trends and observations that can be made about both the broader pools, as well as specific compounds. Both of these provide meaningful information and implications, which will be discussed below.

It is first worth denoting that inorganic P was found to dominate P across nearly all of the samples. This is expected, given that the samples were of sediment. This was also consistent with what was predicted from our bulk XANES analysis, which showed the same indication in the generated spectra, possibly due to the contributions of Ca and Fe.

Regarding the orthophosphate esters, both the monoester and diester pools showed interesting results. For the monoesters, there is both a presence and a large variation in inositol hexakisphosphate (IHP) stereoisomers, specifically with *scyllo*-IHP and *myo*-IHP (phytate), both of which are fairly common in soils. Generally, the IHP stereoisomers are considered to be

relatively stable orthophosphate monoester compounds, though they too can become mobilized under the correct circumstances and hydrolyzed to phytate for algal use, depending on P demand such as the soil having a sufficient concentration of C and or nitrogen (N), or whether the relevant compounds are bound to that of Ca or Fe (Liu, 2017). Accumulation of IHP stereoisomers can occur in soils largely due to the higher sorption capacity from their six phosphate groups, forming relatively stable complexes that are more resistant to degradation, and in some cases even competing with orthophosphate for bonding sites. There was a study that found the primary method by which inositol phosphates enter soil was through catchment runoff, wherein concentrations of IHP were found to be higher in rivers compared to the bay (Suzumura & Kamatani, 1995).

In this study, total IHP concentrations were shown to vary from March to June, albeit inconsistently. This implies a noticeable seasonal influence on the presence of these compounds. This could be because animals have a difficult time breaking down the inositol phosphates and will consequently have relatively large amounts of IHP in their manure (Giles & Cade-Menun, 2005). Therefore the correlated increase in farming activity, and by extension manure spreading, associated with the drier months, could potentially account for the increase in concentration. However, this change in IHP may also be due to the precipitation, as the rainfall has been shown to enable the transfer of organic soil P throughout aquatic system, which in turn will undergo degradation during transport downstream (Condron et al., 2005). There has not been too much research conducted about the transport and transformation of IHP stereoisomers, particularly in these aquatic systems, so these data imply the need for further study.

Looking closer, *myo*-IHP (phytate) showed more consistent variation when compared to that of other stoichiometric forms of IHP, increasing in concentration from March to June. Phytate is an

important organic P compound not readily detectable to those studying soil samples. It is often considered a major storage constituent for P in plant soil (Cosgrove, 1980), and the results suggest a spatial influence, given that the samples from Tintern Abbey samples show virtually no difference in phytate, in contrast to that of the Bunoke site. It is only through use of NMR spectroscopy were we able to detect this level of speciation in the sediment. IHP stereoisomers were more complicated, and required more thorough analysis.

This work found a variety of phospholipids as well. These are commonly detected in river sediments, have been shown to exhibit seasonal and spatial variability (Cade-Menun, 2005). Though the phospholipids were not specifically identified, instead grouped into a category of diester compounds, alongside their degradation compounds, the aforementioned variety can also be seen in the results. Given that orthophosphate diester P forms can be considered to represent the readily labile organic phosphorus pool (Liu, 2017), it is important to note the consistent increase in this group concentration when sampling occurred in June compared to March. However, the concentrations of DNA in particular, shown more clearly in Table A1 displayed in the Appendix, appeared less consistent with that of the orthophosphate diester pool in general, showing little correlation with the sampling period. However, the samples from Bunoke showed higher concentrations than that of Tintern Abbey, suggesting spatial influences. More specially, these sites most likely possess higher levels of microbial growth. This is important when considering that phospholipids may represent microbial activity in terms of a supply of autochthonous matter, such as phytoplankton (Reitzel et al., 2006). Furthermore, DNA has also been shown to increase as a proportion of total organic P as soils age, and is particularly associated with relatively acidic soils (Khanna et al., 1998).

Also of particular interest was the prominent phosphonate peak in the sample BE-Jan19 sample, which was confirmed with spiking to be from the herbicide glyphosate, shown in Figure 4.20 below. Aminomethyl phosphonic acid, a common breakdown product of glyphosate also known as AMPA, was also tested for but not found within the sample. Glyphosate is a chemical component in the herbicide Roundup, commonly used by farmers to control weeds. Indeed, it was later determined that the farmer located upstream the sample catchment site had been spraying Roundup along the fence-line prior to extraction, likely attributing to these results (O'Connell, personal communication). However, glyphosate usually degrades in the sediment and rapidly sorbs within the soil depending largely on acidity of the soil, with higher sorption correlating to a lower pH (Dubbin et al., 2000). Given that glyphosate tends to degrade relatively quickly, and that it was not found in the other samples analyzed, this suggests that the samples were collected soon after the Roundup application.

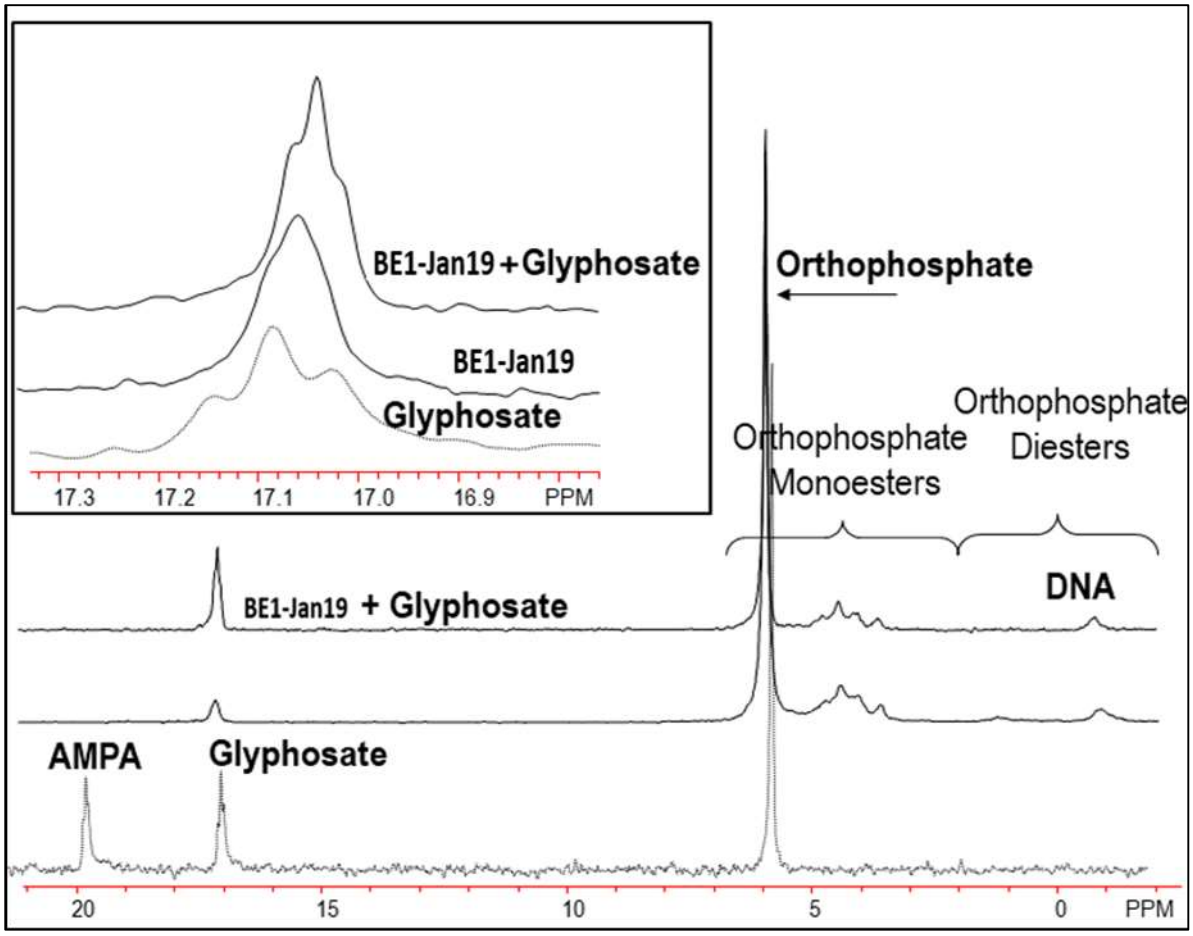

Figure 4.20: ^{31}P NMR Spectra of Glyphosate Spiking Alongside Sample BE1-Jan19

In terms of seasonality, these results agree with the trend noted earlier within the LCF analysis. Namely, that the sampling periods that experience more precipitation, such as March, show more total organic P when compared to the samples recovered in June, as a percentage of total P. The same possible explanations for this correlation outlined in the previous section are still applicable. However, the concentration of every notable species increases in the June samples. Moreover, there was also a consistent increase in both the P forms found in the monoester region and the P forms found in the diester region, when comparing sampling periods from wetter to drier months, possibly due to P transformation between organic and inorganic P. This change can be seen after correcting for the degradation commonly observed during analysis (Cade-Menun,

Navaratnam, Walbridge, 2006). Unsurprisingly, these data then also show the ratio between the two groups remains unaffected when comparing contrasting sampling periods.

There are a number of different processes which act on different time scales, such as vegetation soil coverage or crop management practices, that will go onto affecting the detachment of organic particles, and by extension the aggregate P system stability. A decrease in farming activity may be reasonably attributed to that of the 'wetter' months. Furthermore, with increased precipitation comes an increase in the dilution of P runoff. Though there are also microbial factors to consider as well, as the warmer temperatures will typically see an increase in microbial growth. Moreover, there are also redox conditions to consider as well. It has long since been known that redox conditions, alongside that of temperature and pH, are among the most important environmental factors that dictate P release (Einsele, 1936). A study by Penn et al. in 2000 found that P release rates show a strong seasonal variation when measured across the different redox and pH conditions exhibited annually, and that the P release rates are most accurately represented when measured as a time-weighted, yearly average. Soil redox conditions that contribute to the regulation of biogeochemical transformation of iron bound P vary with seasonality, given that P transformation is affected by the temperature, availability of C sources, and the supply of terminal electron acceptors, and will in turn affect the characterization of P (Mendes, et al., 2018). In addition to the favourable redox conditions provided by the drier months, an increase in the amount of manure applied on farmland, when comparing summer to that of spring, can be seen to increase the expected amount of P runoff, which is then possibly attributed to an increase in the amount of organic P, and by extension, the labile P_o diesters.

Also worth noting is the lack of any notable relationship between molecular P speciation and the intrasite sampling locations. In terms of total organic P, orthophosphate diesters, or any other

notable P forms, there was no significant spatial influence of inflow versus outflow sample collection. This same trend cannot be said about the variation observed between the sampling sites themselves, along with their associated geological and/or soil composition differences, although it is worth noting that this observation cannot be readily made with the NMR sample results alone.

4.3 Comparison of P K-Edge XANES and ^{31}P NMR Results

As outline earlier in this thesis, P K-edge XANES and ^{31}P NMR possess unique and complimentary advantages when used congruently alongside one another for P_i and P_o speciation. Other studies have already proven the limitations of only using a single method to study the cycling of P in terms of speciation (Liu, et al., 2014).

With that said, it is first worth pointing out that there was a relatively small amount of overlap between the two sets of samples, with respect to their sampling sites/periods, in comparison to their individual sections. It is also important to clarify that the LCF spectral fitting was, broadly speaking, underestimating the organic P forms in the samples.

Regardless, it is only by using these methods together that we can fully understand the molecular characterization of the soil samples. This can be seen, at least to some degree within this research as well, wherein the dominance of Fe-P found in the P K-edge XANES LCF analysis, represented as samples with the highest percentage of P in the sample, correlates to the highest Pi found in the extracted P sample for the ^{31}P NMR analysis. Namely, these samples each correspond to that of the Bunoke site, in the June sampling period. Moreover, these same samples also showed the highest P recovery from the NaOH-EDTA extracts, suggesting that the

P extracted was that of associated labile pools, correlating to higher concentrations of insoluble P forms, such as hydroxyapatite or other mineral-linked P groups.

4.4 Results and Discussion Summary

Broadly speaking, the results obtained and discussed in the analysis sections above show several important observations. Through the use of XRF analysis, we are able to see that the samples all appear to be dominated by iron, and though the data can be somewhat inconsistent, a wide variety of elemental distributions are observed among the intra-site locations, sampling sites, and sampling periods, with typically more iron seen in the drier months. The trend of iron dominance was also observed in the XANES analysis sections, both bulk and μ-XANES. However, the sediment samples were found to increase in Fe-linked P compound concentration in the drier months. Lastly, the NMR results, which agreed with the observation made within the LCF analysis of being dominated by inorganic compounds, also found that virtually every P compound identified was seen to increase in the drier months, as opposed to the spring.

5 Conclusions and Recommendations

5.1 Conclusions

This thesis details a comprehensive review of the analytical techniques of X-Ray Fluorescence (XRF) Spectroscopy, X-ray Absorption Near-edge Structure (XANES) spectroscopy, and ^{31}P Nuclear Magnetic Resonance (NMR) spectroscopy, in order to thoroughly understand the molecular speciation of fluvial sediment samples. The data obtained through these techniques demonstrate their complementary nature to one another, and how they can be used as powerful tools in understanding the P characterization of the samples.

Throughout all of the samples analyzed, clear elemental variation can be observed from each technique, with spatial and particularly temporal influences on molecular characterization clearly shown from the advanced spectroscopic methods.

Broadly speaking, there was a significant seasonal influence on speciation, with the summer sampling periods displaying an observable increase in the concentration of Fe-linked P and notable organic P compounds, despite showing consistent decreases the elemental presence of Fe found through XRF analysis. This same trend is observed in the concentrations of orthophosphate monoesters and diesters, including that of DNA, which increased consistently during the summer sampling periods compared to spring. Despite inconsistent variation with respect to total IHP concentrations, phytate was also seen to increase from March to June, if only for the Bunoke site. NMR analysis was also able to show a notable variety in presence of phospholipids, as well as a significant concentration of glyphosate, confirmed by sample spiking, observed in one of the sediment samples.

Spatial differences were also observed, both in terms of site-to-site comparison as well as catchment inflow versus outflow, though the trends in data were relatively inconsistent.

The influence of sediment-associated P from agricultural catchments on fluvial systems needs to be studied further. The variations in molecular characterization observed among the different sampling sites may very well be attributed to the differences in soil composition, especially when considering that temporal disparity among sites is only a major factor with Tintern Abbey, and not between Bunoke and Ballynamona. This is particularly important given that the P had been shown to cause the release of labile orthophosphate diesters, and lead to organic P transformation. The implications of soil composition and the surrounding environment on P speciation needs to be further explored, particularly within fluvial aquatic systems, wherein the P transformation mechanisms are still relatively unknown. The molecular characterization of P compounds, through advanced spectroscopic analysis techniques alongside one another, can be studied in order to show the impact of phosphorus on eutrophication in fluvial environments.

5.2 Recommendations

Although our understanding of molecular level characterization of P in fluvial soils has benefited greatly from the use of the advanced methods outline in this thesis, there is still a lot more that can be done. In order to better study the soil P speciation, it is recommended to improve the consistency of the sample selection in terms of the two different spectroscopic methods. Because the samples did not line up perfectly with one another in terms of extraction dates, and site locations, it was difficult to isolate particular parameters and a certain degree of extrapolation was required. Increasing the sample set size is also always beneficial. More to this point, the

more accurately the soil P composition in each sample can be represented, the better the speciation data can serve to provide source tracing and appropriate modelling mechanisms. Moreover, there are several microscopic imaging techniques, such as that of Raman spectroscopic mapping, which would provide a great amount of structural detail for organic function groups within the soil samples which could prove invaluable towards the modelling mechanisms developed in future research.

References

Ansari, A. & Singh, G. *Eutrophication: Causes, Consequences and Control*, 2011

Blaise, D, Venugopalan, M, Singh, G, *Phosphorus Management*. Textbook of Plant Nutrient Management, 93-121, 2018

Cade-Menun, B.J. & Preston, C.M. *A Comparison of Soil Extraction Procedures for 31P NMR Spectroscopy,* Soil Science 11, 770-85, 1996

Cade-Menun, B.J., *Characterizing phosphorus in environmental and agricultural samples by 31P nuclear magnetic resonance spectroscopy*, Talanta, 66:2, 359-371, 2005

Cade-Menun, B.J., Navaratnam, J, Walbridge, M, *Characterizing Dissolved and Particulate Phosphorus in Water with 31P Nuclear Magnetic Resonance Spectroscopy*, Environmental Science & Technology, 40, 7874-7880, 2006

Canet, D., *Nuclear Magnetic Resonance: Concepts and Method*, 1996

Central Statistics Office (CSO), *Environmental Indicators Ireland 2016*, 2016

Condron, M., Turner, B, Cade-Menun, B, Sims, J, *Chemistry and Dynamics of Soil Organic Phosphorus, Phosphorus: Agriculture and the Environment*, 2005

Corbridge, D.E.C.. *Phosphorus 2000. Chemistry, biochemistry & technology*. Elsevier, 2000

Cosgrove, D. J., *The Determination of Myo -inositol Hexakisphosphate phytate*, Journal of the Science of Food and Agriculture 31.12, 1253-256, 1980

DePinto, J. V., Young, T, Martin, S, *Algal-available Phosphorus in Suspended Sediments from Lower Great Lakes Tributaries*. Journal of Great Lakes Research, 7, 311-325, 1981

Dubbin, W.E., Sposito, G, Zavarin, M, *X-ray absorption spectroscopic study of Cuglyphosate adsorbed by microcrystalline gibbsite*, Soil Science, 165:699–707, 2000

Dubrovsky, N.M., Burow, K, Clark, G, Gronberg, J, Hamilton, P, Hitt, K, Mueller, D, Munn, M, Nolan, B, Puckett, L, Rupert, M

Terry M. Short, Norman E. Spahr, Lori A. Sprague, and William G. Wilber. *The quality of our Nation's waters—Nutrients in the Nation's streams and groundwater*, 1992–2004: U.S. Geological Survey Circular 1350, 174, 2010

Einsele, W., *Uber die Beziehungen des Eisenkreislaufs zum Phosphatkreislauf im eutrophen Seen*, Archives of Hydrobiology, 29, 664–686, 1936

Environmental Protection Agency, *Analysis of the Sources of Phosphorus in the Environment*, Toxic Substances, 1979

Environmental Protection Agency, *Guidance for Developing Ecological Soil Screening Levels*, OSWER Directive 9285.7-55, 2003

Environmental Protection Agency, *Water Quality in 2017: An Indicators Report*; Environment Protection Agency of Ireland, 2018

Food and Agriculture Organization, *The state of the world's land and water resources for food and agriculture (SOLAW) – Managing systems at risk. Food and Agriculture,* 2011

Food and Agriculture Organization and World Health Organization, *Assessment of the State of Eutrophication in the Mediterranean Sea*, United Nations Environment Programme, 1995

Geological Survey of Ireland, *Groundwater Newsletter Issue 33 May 1998*, 1998

Giles, C. D., Cade-Menun, B, Hill, J, *The inositol phosphates in soils and manures: abundance, cycling, and measurement*, Can. J. Soil Science, 2011

Glaesner, N., Van Der Bom, F, Bruun, S, McLaren, T, Larsen, F, Magid, J, *Phosphorus characterization and plant availability in soil profiles after long-term urban waste application*. Geoderma. 338. 136-144. 10.1016, 2019

Gu, C., Hart, S, Turner, B, Hu, Y, Meng, Y, Zhu, M, *Aeolian dust deposition and the perturbation of phosphorus transformations during long-term ecosystem development in a cool, semi-arid environment*. Geochimica et Cosmochimica Acta, 246, 498-514, 2019

Gustafsson, J, Braun, S, Tuyishime, J, Adediran, G, Warrinnier, R, Hesterberg, D, *A Probabilistic Approach to Phosphorus Speciation of Soils Using P K-Edge XANES Spectroscopy with Linear Combination Fitting,* Soil Systems 2020, 4, 26, 2020

Hawkes, G.E., Powlson, S, Randall, E, Tate, K, *A 31P nuclear magnetic resonance study of the phosphorus species in alkali extracts of soil from long-term field experiments*. J. Soil Sci. 35:35–45, 1984

Hesterberg, D., McNulty, I, Thieme, J, *Speciation of Soil Phosphorus Assessed by XANES Spectroscopy at Different Spatial Scales*. United States: N., 2017

Jennings, E. Mills, P, Jordan, P, Jensen, J, *Eutrophication from Agricultural Sources: Seasonal Patterns & Effects of Phosphorus,* Environmental Protection Agency, 2003

Jensen, H. S., & Thamdrup, B, *Iron-bound phosphorus in marine sediments as measured by bicarbonate-dithionite extraction*. Hydrobiologia, 253 1-3, 47-59, 1993

Kelly, S. D. Hesterberg, D, Ravel, B, *Analysis of Soils and Minerals Using X-ray Absorption Spectroscopy, Soil Science Society of America*, 677 Methods of Soil Analysis, 2005

Khanna, M., Yoder, M, Calamai, L, Stotzky, G, *X-ray diffractometry and electron microscopy of DNA from Bacillus subtilis bound on clay minerals*, Science Soils 3: 1–8, 1998

Kulaev, I.S., *The biochemistry of inorganic polyphosphates*. John Wiley & Sons, 1979

Kuo, S., *Phosphorus. Methods of soil analysis. Part 3. Chemical methods*, SSSA, 1996

Liu, J. Cade-Menun, B, Yang, J, Liang, X, *Molecular speciation of phosphorus present in readily dispersible colloids from agricultural soils*. Soil Science Society American Journal 78, 47–53, 2014

Liu, Yang, J, Cade-Menun, B, Hu, Y, Li, J, Peng, C, Ma, Y, *Molecular speciation and transformation of soil legacy phosphorus with and without longterm phosphorus fertilization: Insights from bulk and microprobe spectroscopy*, Scientific Reports 7, 15354, 2017

McDowell, R. W., Mahieu, N, Brookes, P, Poulton, P, *Mechanisms of phosphorus solubilisation in a limed soil as a function of pH*, Chemosphere 51, 685–692, 2003

McDowell, R.W., Stewart, I, Cade-Menun, B, *An examination of spin–lattice relaxation times for analysis of soil and manure extracts by liquid state phosphorus-31 nuclear magnetic resonance spectroscopy*, J. Environ. Qual. 35, 293-302, 2006

Mendes, L., Tonderski, K, Kjaergaarda, C, *Phosphorus Accumulation and Stability in Sediments of Surface-flow Constructed Wetlands*, Geoderma 331: 109-20, 2018

Mishra, K. R., Thomas, S, Thomas, R, Zachariah, A, *Spectroscopic Methods for Nanomaterials Characterization*, 369-415, 2017

Murphy, J. & Riley, J. P. *A modified single solution method for determination of phosphate in natural waters*, Analytica Chimica Acta 27:31–36, 1962

Ngatia, L. & Taylor, R. *Phosphorus Eutrophication and Mitigation*, Phosphorus - Recovery and Recycling, 2018

Ortiz-Reyes, E., & Anex, R. P. *A life cycle impact assessment method for freshwater eutrophication due to the transport of phosphorus from agricultural production*. Journal of Cleaner Production, 177, 474-482, 2018

Penn, Michael R. Auer, M, Doerr, S, Driscoll, C, Brooks, C, Effler, S, *Seasonality in phosphorus release rates from the sediments of a hypereutrophic lake under a matrix of pH and redox conditions*, Can. J. Fish. Aquatic Science 57: 1033-1041, 2000

Piezynski, McDowell, R, Sims, T, *Chemistry, Cycling, and Potential Movement of Inorganic Phosphorus in Soils*, Phosphorus: Agriculture and the Environment, 2005

Poly, F., Chenu, C, Simonet, P, Rouiller, J, Monrozier, L, *Differences between linear chromosomal and supercoiled plasmid DNA in their mechanisms and extent of adsorption on clay minerals*. Langmuir 16:1233–1238, 2000

Ravel, B., & Newville, M., *ATHENA, ARTEMIS, HEPHAESTUS: data analysis for X-ray absorption spectroscopy using IFEFFIT*, Journal of Synchrotron Radiation 12, 537–541, 2005

Regan, J.T., Fenton, O, Healy, M, *A REVIEW OF PHOSPHORUS AND SEDIMENT RELEASE FROM IRISH TILLAGE SOILS, THE METHODS USED TO QUANTIFY LOSSES AND THE CURRENT STATE OF MITIGATION PRACTICE*, Biology and Environment: Proceedings of the Royal Irish Academy 112B.1 157-83, 2012

Reitzel, K., Ahlgren, J, Gogoll, A, Jensen, H, Rydin, E, *Characterization of phosphorus in sequential extracts from lake sediments using 31P nuclear magnetic resonance spectroscopy*, Canadian Journal of Fisheries and Aquatic Sciences, 63(8): 1686-1699, 2006

Schindler, D. W. *Eutrophication and Recovery in Experimental Lakes: Implications for Lake Management*, Science, vol. 184, no. 4139, 897–899, 1974

Shang, C., Huang, P, Stweart, J, *Kinetics of adsorption of organic and inorganic phosphates by short-range ordered precipitate of aluminum*. Can. J. Soil Science 70:461–470, 1990

Sharpley, A. & Tunney, H., *Phosphorus Research Strategies to Meet Agricultural and Environmental Challenges of the 21st Century*, Journal of Environmental Quality 29.11 76-81, 2000

Shiau, Y., Pai, C, Tsai J, Liu, W, Yam, R, Chang, S, Tang, S, Chiu, C, *Characterization of Phosphorus in a Toposequence of Subtropical Perhumid Forest Soils Facing a Subalpine Lake*, Forests 2018, 9, 294, 2018

Shore, M.M, Murphy, S, Mellander, P, Shortle, G, Melland, A, Crockford, L, O'Flaherty, V, Williams, L, Morgan, G, Jordan, P, *Influence of stormflow and baseflow phosphorus pressures on stream ecology in agricultural catchments*, Sci. Total Environ., 590–591, 469–483, 2017

Simpson, A, Simpson, M, Soong, R, *Environmental Nuclear Magnetic Resonance Spectroscopy: An Overview and a Primer*, Analitical Chemistry 90, 628−639, 2018

Søndergaard, M., Jeppesen, E, Lauridson, T, Skov, C, Van Nes, G, Roijackers, R, Lammens, E, Portielje, R, *Lake Restoration: Successes, Failures and Long-term Effects*, Journal of Applied Ecology 44.6, 1095-105, 2007

Suzumura, M. & Kamatani, A., *Origin and distribution of inositol hexaphosphate in estuarine and coastal sediments*, Limnol. Oceanogr, 40, 1254, 1995

USEPA (U.S. Environmental Protection Agency), *National Summary of State Information.* U.S. Environmental Protection Agency, Office of Water, Office of Wetlands, Oceans and Watersheds, Washington, 2016

Wei, Changfu, Tian, H, Wei, H, Yan, R, Chen, P, *An NMR-Based Analysis of Soil–Water Characteristics*. Applied Magnetic Resonance 45.1, 49-61, 2014

Werner, F. & Prietzel, J., *Standard Protocol and Quality Assessment of Soil Phosphorus Speciation by P K -Edge XANES Spectroscopy*. Environmental science & technology, 49, 2015

Vero, S., Daly, K, McDonald, N, Leach, S, Sherriff, S, Mellander, P, *Sources and Mechanisms of Low-Flow River Phosphorus Elevations: A Repeated Synoptic Survey Approach*, *Water (Basel)* 11.7 1497, 2019

Young, E.O., Ross, D, Cade-Menun, B, Liu, C, *Phosphorus speciation in riparian soils: A phosphorus-31 nuclear magnetic resonance spectroscopy and enzyme hydrolysis study*. Soil Science Society American Journal 77, 1636–1647, 2013

Zhang, Qingxin, *Speciation of Bioavailable Phosphorus in Fluvial Sediments*, MSc Thesis, University of Saskatchewan, Chemical Engineering, 2020

Zhang, X, Ade, H, Jacobson, C, Kirz, J, Lindaas, S, Williams, S, Wirik, S, *Micro-XANES: Chemical Contrast in the Scanning Transmission X-ray Microscope*, Nuclear Instruments and Methods in Physics Research A 347, 1994

Appendix

The first table in included in the Appendix (A.1) provides the specific compound pools identified through the use of NMR Spectroscopy, while the second shows the corresponding chemical shifts associated with the analyzed samples. The Figures thereafter show the LCF reference standards and the respective sample sites from the XANES analysis.

Table A.1: ^{31}P NMR Total Distribution Results Summary (µg/g)

ID	OrthoP	Pyro	Poly	Phn	17ppm	myoIHP	ScyIHP
BE3-Mar19	530.5	11.9	19.6	12.8	0.0	23.8	17.9
BE3-Jun19	1232.7	51.4	47.6	13.3	0.0	78.0	39.9
BE2-Mar19	540.4	17.2	32.6	13.4	0.0	40.2	20.1
BE2-Jun19	1190.5	40.1	36.6	26.1	0.0	78.4	26.1
BE1-Jun19	1592.3	39.8	46.8	16.4	0.0	105.4	16.4
BE1-Mar19	174.2	4.6	11.3	4.1	0.0	10.7	5.5
BE1-Jan19	90.3	2.4	6.7	2.4	4.4	3.9	2.9
TTA-Nov17	93.3	4.5	4.0	3.5	0.0	9.1	7.6
TTA-Jun18	120.4	3.7	7.7	1.5	0.0	5.2	3.9
TTA-Sep17	231.6	5.4	5.4	2.2	0.0	8.3	4.1

neoIHP	ChiroIHP	α-glyc	β-glyc	Nucl	Pchol	g6P	5 ppm	Mono1	Mono2	Mono3
6.0	11.9	6.0	11.9	46.8	6.0	6.0	11.9	11.9	46.8	11.9
13.3	53.3	26.6	51.4	64.7	13.3	13.3	13.3	26.6	51.4	13.3
6.7	13.4	13.4	26.8	33.5	6.7	6.7	6.7	13.4	39.3	13.4
12.2	24.4	26.1	38.3	38.3	12.2	12.2	12.2	26.1	66.2	12.2
16.4	51.5	23.4	51.5	105.4	16.4	16.4	16.4	35.1	105.4	16.4
1.7	3.5	3.8	7.3	10.7	1.7	1.7	3.8	5.5	18.3	3.8
1.0	2.0	2.0	3.9	10.9	1.0	1.0	2.0	1.0	11.9	1.0
1.5	9.1	4.5	9.1	43.5	1.5	1.5	1.5	7.6	15.2	6.1
1.2	2.5	2.7	5.2	10.4	1.2	1.2	2.7	5.2	13.1	1.2
2.2	4.4	2.2	4.1	8.3	2.2	1.0	2.2	6.3	12.1	2.2

DNA	OthDi1	OthDi 2	Total
31.5	20.4	5.1	850.1
57.1	28.5	13.3	1902.3
52.7	43.1	18.2	958.2
20.9	33.1	10.5	1743.0
18.7	39.8	11.7	2341.7
6.1	9.9	2.0	290.3
6.4	4.7	1.3	163.1
10.6	15.9	3.0	252.7
9.5	7.5	1.5	207.6
2.9	8.9	1.3	317.3

Table A.2: Chemical shifts of peaks detected in ^{31}P-NMR spectra

Category	P Form or Compound Class	Chemical Shift (ppm)
Inorganic P		
	Orthophosphate	6.00 ± 0.00
	Pyrophosphate	-4.18 ± 0.09
	Polyphosphates	-4.03 ± 0.07, -4.59 ± 0.18, -5.65 ± 0.64, -6.29 ± 0.23, -8.15 ± 0.64, -9.41 ± 0.17, -10.83 ± 0.67, -11.99 ± 0.68, -14.02 ± 0.68, -15.41 ± 0.54, -17.29 ± 0.52, -18.59 ± 0.27, -19.12 ± 0.08, -19.99 ± 0.25, -20.84 ± 0.11, -21.43 ± 0.43, -22.43 ± 0.32, -23.37 ± 0.22 , -24.38 ± 0.19 , -26.17 ± 0.66
Organic P		
	Phosphonates	28.53 ± 0.32 27.38 ± 0.34, 26.27 ± 0.37, 24.90 ± 0.58, 23.44 ± 0.30, 22.31 ± 0.65, 21.12 ± 0.47, 19.43 ± 0.38, 18.71 ± 0.33, 17.59 ± 0.28, 15.85 ± 0.72, 14.32 ± 0.60, 12.41 ± 0.50, 11.26 ± 0.52, 9.48 ± 0.38, 8.24 ± 0.41
	Orthophosphate Monoesters	
	myo-IHP	5.50 ± 0.04, 4.57 ± 0.05, 4.16 ± 0.06, 4.08 ± 0.04
	scyllo-IHP	3.72 ± 0.05
	neo-IHP	6.35 ± 0.05, 4.40 ± 0.07
	D-*chiro*-IHP 4e/2a	6.55 ± 0.03, 5.30 ± 0.05, 3.97 ± 0.05
	D-*chiro*-IHP 4a/2e	6.26 ± 0.02, 4.71 ± 0.06, 4.29 ± 0.05
	Glucose 6-phosphate	5.23 ± 0.05
	α-glycerophosphate	4.85 ± 0.06
	ß-glycerophosphate	4.51 ± 0.04
	Mononucleotides	4.51 ± 0.05, 4.46 ± 0.01, 4.42 ± 0.02, 4.37 ± 0.02, 4.30 ± 0.01, 4.27 ± 0.00, 4.23 ± 0.01, 4.18 ± 0.01
	Choline phosphate	3.86 ± 0.04
	Unknown 5 ppm	4.96 ± 0.05
	Monoester 1	7.19 ± 0.06, 7.05 ± 0.05, 6.90 ± 0.06, 6.78 ± 0.06, 6.62 ± 0.07, 6.40 ± 0.06
	Monoester 2	5.80 ± 0.05, 5.72 ± 0.02, 5.57 ± 0.04, 5.31 ± 0.08, 5.10 ± 0.08, 4.97 ± 0.10, 4.76 ± 0.042, 4.65 ± 0.04
	Monoester 3	3.66 ± 0.07, 3.56 ± 0.02, 3.45 ± 0.03, 3.36 ± 0.03, 3.15 ± 0.05, 2.96 ± 0.05, 2.85 ± 0.05, 2.70 ± 0.06
	Orthophosphate Diesters	
	Other Diester 1	2.29 ± 0.07, 2.09 ± 0.07, 1.62 ± 0.03, 1.44 ± 0.07, 1.26 ± 0.05, 1.10 ± 0.08, 0.84 ± 0.08, 0.63 ± 0.05, 0.24 ± 0.06, 0.09 ± 0.07, -0.18 ± 0.11, -0.49 ± 0.11,
	DNA	-0.71 ± 0.06, -0.94 ± 0.06
	Other Diester 2	-1.09 ± 0.08, -1.22 ± 0.03, -1.48 ± 0.08, -1.67 ± 0.05, -1.89 ± 0.09, -2.49 ± 0.15 -2.97 ± 0.22, -3.48 ± 0.17

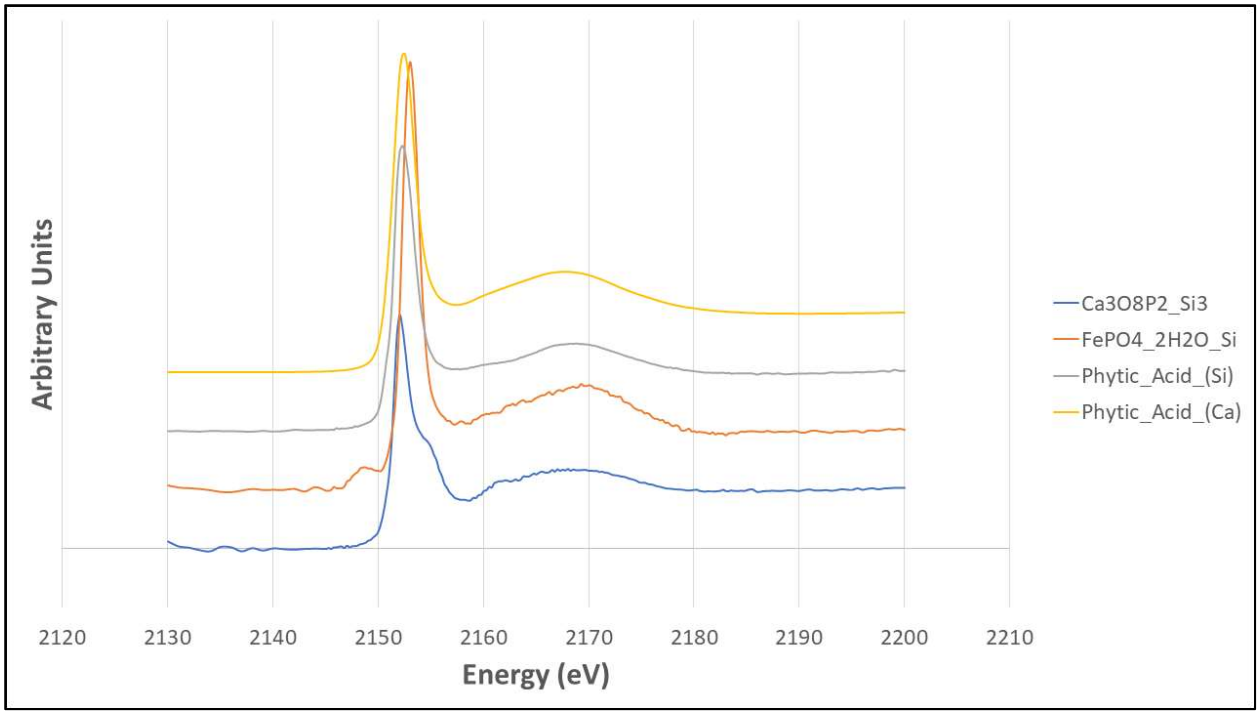

Figure A.1: LCF Reference Standard XANES Spectra

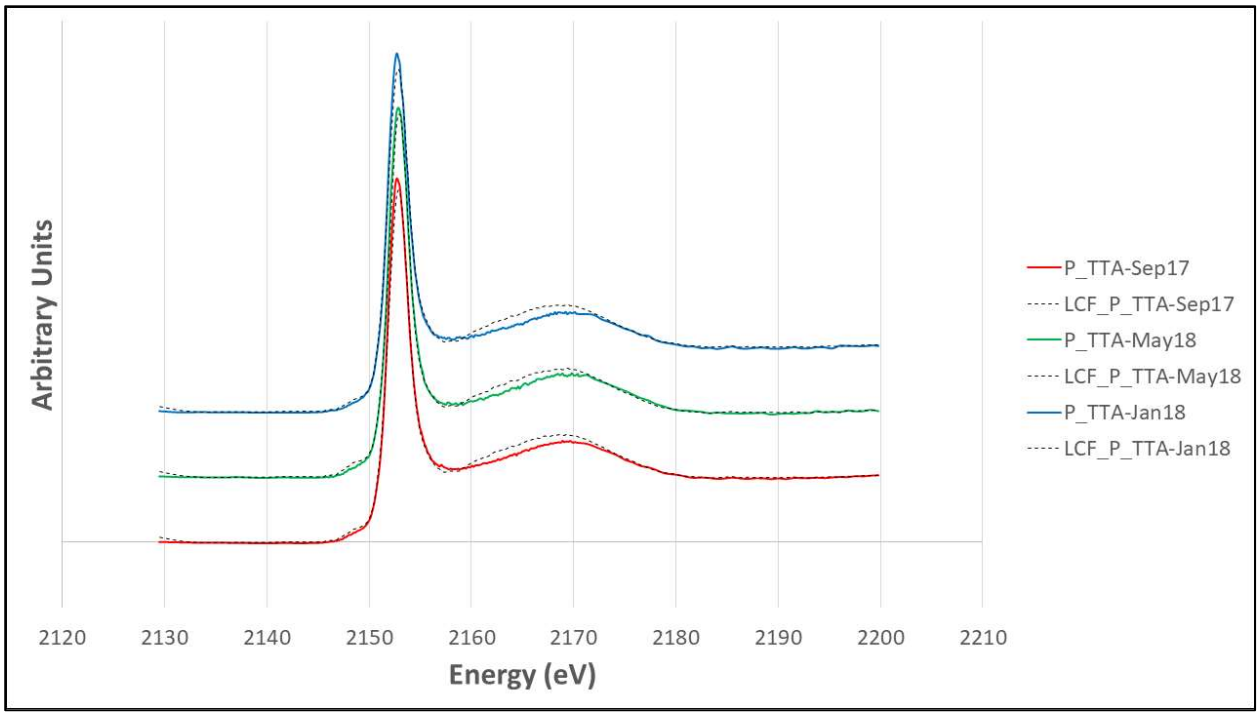

Figure A.2: LCF XANES Spectra for Tintern Abbey

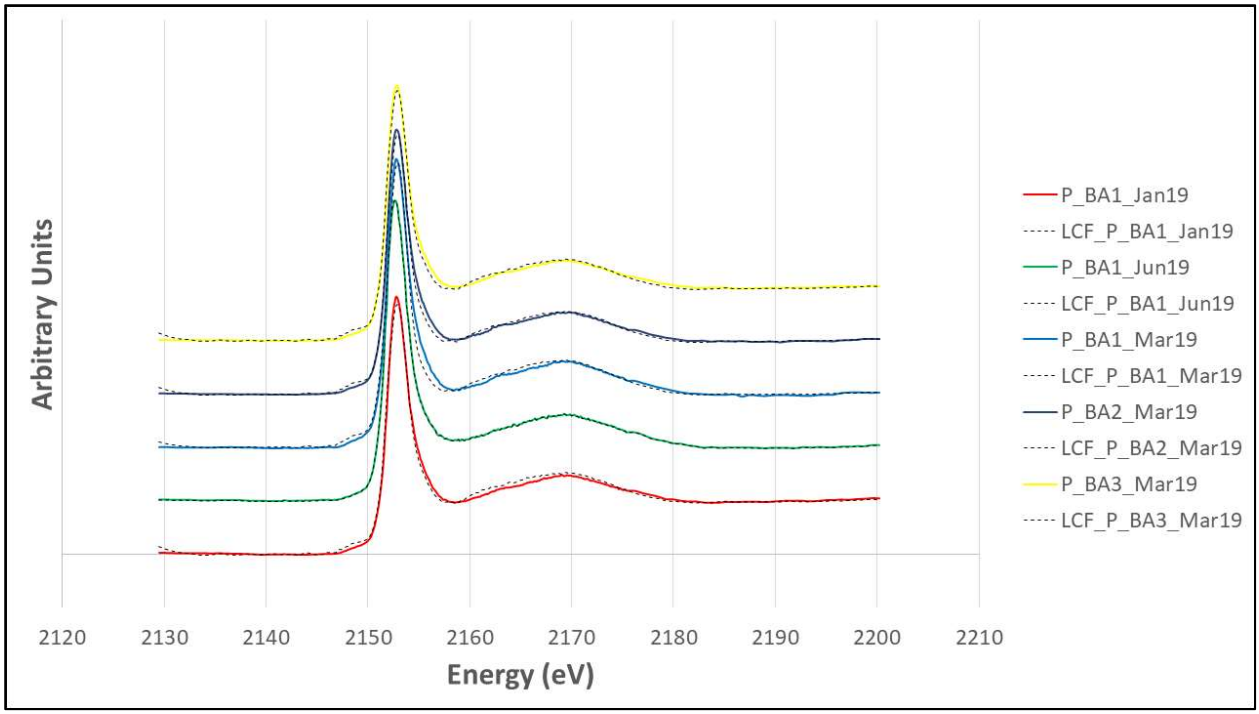

Figure A.3: LCF XANES Spectra for Ballynamona

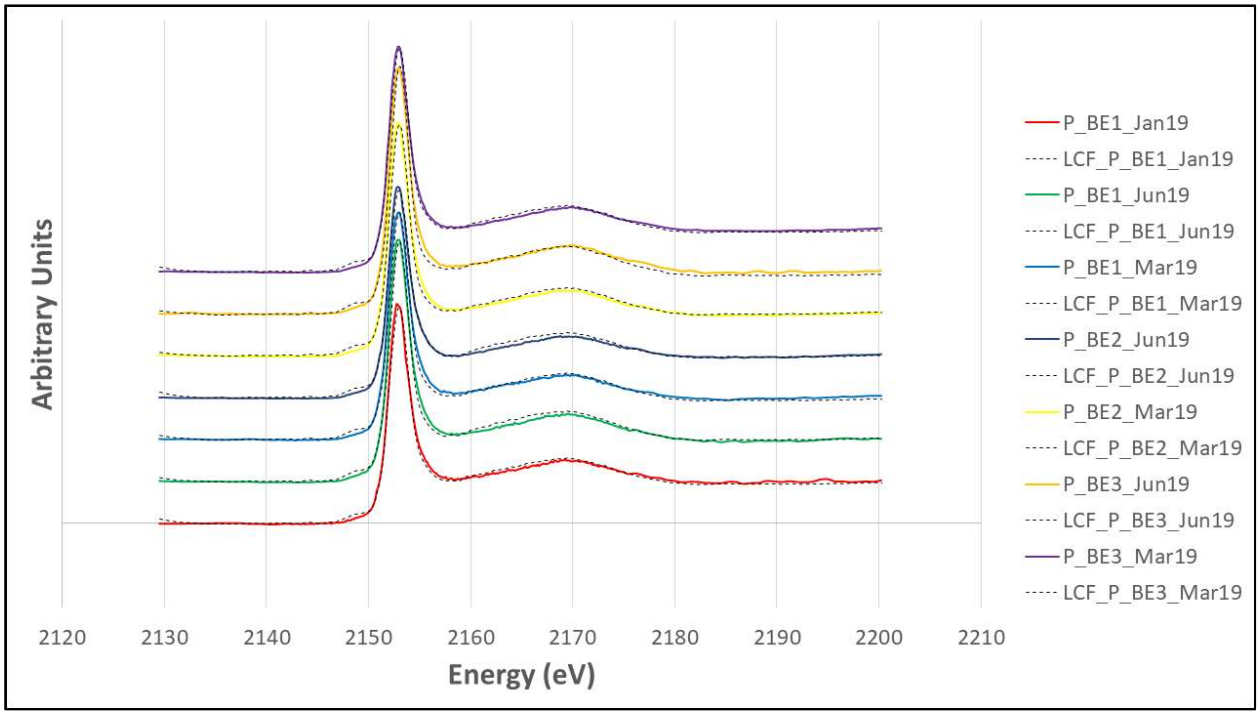

Figure A.4: LCF XANES Spectra for Bunoke

Sampling procedure for Eutro-SED project:

At the selected catchment sites, stream suspended fluvial sediment was collected using time integrated sediment traps, at the outflow intra-site locations. These traps were installed horizontally in the middle of the actual stream flow and set up at approximately 60% of the average water depth through an apparatus of steel uprights and plastic cable ties to steel rebar, which was installed deep inside of the channel. These sediment traps were deployed periodically over the course of a particular time period, typically at after the case of a high-flow event, such as a storm or heavy rainfall.

After fluvial soil deposition was observed, these traps were carefully removed from the streams and transferred into sterile, 10L containers. These containers were stored nearby, and kept at a temperature equal to, or as close as possible to, the stream temperature, even whilst being transported back to the laboratory, wherein the sediments were stored in a refrigerator and processed through wet sieving the fluvial sediment via 63µm steel stainless sieves, as well as centrifugation at 5000 rpm, and the supernatant being decanted. Finally, the samples are then freeze-dried for further experiments and future analysis.